***Interactive comment on*** **"Estimating spatially distributed soil water content at small watershed scales based on decomposition of temporal anomaly and time stability analysis"** ***by*** **W. Hu and B. C. Si**

**Anonymous Referee #1**

Received and published: 4 August 2015

Manuscript hessd-12-6467-2015 introduces an empirical orthogonal function (EOF) approach for analysing spatio-temporal patterns in soil water content observations. The presented approach is similar to other principal component analyses recently applied to spatio-temporally resolved geo-data. The approach may be seen as an extension to the one presented by Parry and Niemann (2007), a reference that is frequently cited in the manuscript. Parry and Niemann (2007) first extract the spatial arithmetic average soil water content from the 2-D spatio-temporally resolved measurement data. They then apply an EOF on the residuals which are consequently split into expansion coefficients (ECs, i.e. the eigenvectors of the space-time matrix of residuals) and empirical orthogonal functions (EOFs, i.e. the residuals mapped on the eigenvectors). EOFs may then be used to identify regions with similar hydrologic behaviour or to down-scale average water contents of the entire region. The novelty of the approach presented in hessd-12-6467-2015 is that first the temporal arithmetic average is subtracted from the data as in Mittelbach and Seneviratne (2012, also frequently cited). In a next step, the spatially constant fraction is isolated from the residuals. The EOF is then only applied on the residuals of the residuals. The authors discuss cases in which their approach has advantages over the one of Perry and Niemann (2007) and demonstrate that their approach yields water content better cross-correlation results for a dataset collected long a transect in the Canadian prairies.

The manuscript hessd-12-6467-2015 is in an already well developed state which made it relatively easy to read. As far as I can judge the English is good with only a few exception missing articles and occasional strange wording. The manuscript is largely well-structured albeit that I think that the manuscript would gain if the discussion on when the here presented EOF approach is advantageous (P6484,L12 – P6485,L23) was moved to the material and method section. As the authors write on P6484,L16 and L23, most of the text in these three paragraphs is founded on theory and is known a priori. I think it would make it easier to understand the new approach if the circumstances under which it is advantageous would already be quantitatively explained in the material and methods section. Moreover, the discussion section could be improved by better separating discussions i) on correlations between site factors and time events with model parameters (e.g. M_tn or EOF1) and ii) on prediction performance of the model. Also, the conclusions are more of a summary in its present state.

Response:

Thank you for reviewing our manuscript and your positive and constructive comments. Please refer to all changes in the revised manuscript following our response.

(1) We have checked the English carefully again, and we also had a colleague checked the language. The required articles were added.

(2) We moved the discussion on situations that the TA model is advantageous in theory into the material and method on Lines 286-308 immediately after introducing the NSCE to evaluate the quality of estimation of spatially distributed SWC. We believe the following three aspects affect the relative performance of the TA model over the SA model: the amount of $R_{tn}$ variance considered in the TA model, the degree of non-linearity between the $M_{\hat{t}n}$ and EOF1 of the $R_{tn}$, and the estimation accuracy of the $\mathrm{EC}_t$ from the cosine function (Eq.4).

Therefore, we changed it as " **Many factors may affect the relative performance of spatially distributed SWC estimation between the TA model and the SA model. First, the degree of outperformance of the TA model over the SA model may depend on the amount of $R_{tn}$ variance considered in the TA model. On one hand, the two models are identical if variance of $R_{tn}$ is close to zero or there are negligible interactions between the spatial and temporal components (Fig. 1). On the other hand, if no underlying spatial patterns exist in the $R_{tn}$ or the underlying spatial patterns contributed little to the total variance of the $R_{tn}$, the outperformance will be also very limited. Therefore, the greater the variance of $R_{tn}$ can be considered in the TA model, the more likely the TA model can outperform the SA model. Second, the way of EOF decomposition may also affect the relative performance. In the SA model, EOF decomposition is performed on lumped time-stable patterns $M_{\hat{t}n}$ and space-variant temporal anomaly $R_{tn}$ (Perry and Niemann, 2007). In the TA model, however, EOF decomposition is made only on $R_{tn}$. In theory, the two models will be identical if $M_{\hat{t}n}$ and the first underlying spatial pattern (i.e., EOF1) of the $R_{tn}$ were perfectly correlated. If a nonlinear relationship exists between them, lumping $M_{\hat{t}n}$ and $R_{tn}$ together, as in the SA model, would weaken the model performance as compared to the TA model. From this aspect, the greater deviation from a linear relationship between the $M_{\hat{t}n}$ and EOF1 of the $R_{tn}$, may lead to a greater outperformance of the TA model over the SA model. Finally, the**

**performances of both models rely on the estimation accuracy of the $EC_t$ which depends on both goodness of fit of the cosine function (i.e., Eq. 4) and estimation accuracy of the $S_{t\hat{n}}$. Because the same $S_{t\hat{n}}$ values are used for the two models, the relative performance of the two models is related to the goodness of fit of Eq. (4). "**

Meanwhile, we also discussed the three factors that can influence the model performance by considering the real situation of our datasets, which can deepen our understanding of the model performance. We put this discussion in to "4.2 Model performance for spatially distributed SWC estimation" (Line 536-610). We changed this part as:

**" 4. 2 Model performance for spatially distributed SWC estimation**

**The outperformance of the TA model for estimating spatial SWC at the Canadian site and Chinese site can be partly explained by the high contribution percentages (average of 19–118%) of the $\sigma^2_{\hat{n}}(R_{tn})$ to the total variance. When SWC is close to average levels, $R_{tn}$ is also close to zero, resulting in negligible variance contribution from $R_{tn}$ to the total variance. In this case, the soil water patterns are stable, the SA model performs well, and there will be little differences between these two models. As is well known, the spatial patterns in soil water contents are inherently time unstable. For example, when evapotranspiration becomes the dominant process at the small watershed scale, more water will be lost in depressions due to the denser vegetation than on knolls (Millar, 1971; Biswas et al., 2012), effectively diminishing the spatial patterns and increasing temporal instability. In this case, the $\sigma^2_{\hat{n}}(R_{tn})$ contributes more to the total variance (e.g., high up to 632%) and the TA model may outperform the SA model. This explained why the outperformance of TA model was more obvious in the dry conditions. For the GENCAI network in Italy, although the $\sigma^2_{\hat{n}}(R_{tn})$ contributed 68% of the total variance, the performance of the TA model was identical to the SA model. This was because there were no underlying spatial patterns in the $R_{tn}$. Similarly, because the first underlying spatial pattern (i.e., EOF1) explained greater percentages of the $\sigma^2_{\hat{n}}(R_{tn})$ at the Canadian site (44–61%) than the Chinese site (23%), the outperformance of the TA model over the SA model was more obvious at the former site (Fig. 9 and 10a). Therefore, the TA model is advantageous only if**

**the contribution of $\sigma^2_{\hat{n}}(R_{tn})$ to the total variance is substantial and underlying spatial patterns exist in the $R_{tn}$.**

**The existence of underlying spatial patterns in the $R_{tn}$ is related to the controlling factors, which may be scale-specific. At small scales, "static" factors such as the depth to the $CaCO_3$ layer and SOC at the Canadian site may affect not only the time-stable patterns but also the $R_{tn}$. The persistent influence of "static" factors on the $R_{tn}$ resulted in significant underlying spatial patterns in the $R_{tn}$. Thus, the TA model outperformed the SA model at the small scales. At large scales such as basin scale or greater, time-stable patterns may be controlled by, in addition to soil and topography (Mittelbach and Seneviratne, 2012), the climate gradient (Sherratt and Wheater, 1984); at those scales, $R_{tn}$ is more likely to be controlled by the meteorological anomaly (i.e., spatially random variation) (Walsh and Mostek, 1980), and the effects of soil and topography may be reduced. Consequently, spatial patterns in the $R_{tn}$ may be weakened and the TA model may have no advantages over the SA model such as for the Italian site.**

**The $M_{\hat{t}n}$ and the underlying spatial patterns (EOF1) in the $R_{tn}$ were controlled by the same spatial forcing (e.g., depth to $CaCO_3$ layer and SOC) at the Canadian site (Table 1), and they were correlated with an $R^2$ of 0.83 for the near surface and 0.42 for the root zone. Although the relationships between $M_{\hat{t}n}$ and $R_{tn}$ were strong, they were not strictly linear, suggesting that $M_{\hat{t}n}$ and $R_{tn}$ were affected differently by these factors. Therefore, the nonlinear relationship between $M_{\hat{t}n}$ and $R_{tn}$ partially contributed to the outperformance of the TA model over the SA model.**

**The relationship between the $S_{t\hat{n}}$ and EC1 was better fitted by the cosine function in the TA model than the SA model (Figs. 4b and 6b), with $R^2$ of 0.76 versus 0.73 in the near surface and 0.88 versus 0.73 in the root zone. The reduced scatter in the $S_{t\hat{n}}$ and EC1 relationship in the TA model may also partly explain the outperformance of the TA model over the SA model.**

**Therefore, the outperformance of the TA model over the SA model depends on counterbalance among the variance of $R_{tn}$ explained in the TA model, the linear**

**correlation between the $M_{\hat{tn}}$ and EOF1 of the $R_{tn}$, and the goodness of fit for the $S_{\hat{tn}}$ and EC1 relationship. For example, the variance of EOF1 in the $R_{tn}$ for the near surface (i.e., 264%$^2$) was much greater than that for the root zone (i.e., 43%$^2$). However, $M_{\hat{tn}}$ and underlying spatial patterns (EOF1) in the $R_{tn}$ in the root zone deviated more from a linear relationship, and the reduced scatter in the $S_{\hat{tn}}$ and EC1 relationship in the TA model was more obviously in the root zone than in the near surface. As a result, the outperformance of the TA model was comparable between the near surface and root zone at the Canadian site (Fig. 9).**

**In the real world, the relations between the $M_{\hat{tn}}$ and underlying spatial patterns in the $R_{tn}$ may rarely be perfectly linear. Therefore, when underlying spatial patterns exist in the $R_{tn}$ and the $R_{tn}$ has substantial variances, the TA model is preferable to the SA model for the estimation of spatially distributed SWC. Because the TA model was not worse than the SA model for the whole range of SWC, the TA model is suggested for the estimation of spatially distributed SWC at different soil water conditions.**

**Previous studies on SWC decomposition mainly focus on near surface layers (Jawson and Niemann, 2007; Perry and Niemann, 2007, 2008; Joshi and Mohanty, 2010; Korres et al., 2010; Busch et al., 2012). This study decomposed spatiotemporal SWC using the TA model for both the near surface and the root zone. The results showed that the estimation of spatially distributed SWC at small watershed scales was improved by the TA method that considers the $R_{tn}$. Because of the stronger time stability of SWC in deeper soil layers (Biswas and Si, 2011), SWC evaluation in thicker soil layers was more accurate than in shallow soil layers. This is particularly important because SWC data for deeper soil layers in a watershed is more difficult to collect than that of surface soil."**

**(3) We separated the discussion into two parts:**

**4.1 Controls of the $M_{\hat{tn}}$ and $R_{tn}$**

**4. 2 Model performance for spatially distributed SWC estimation**

(4) We changed the conclusions to make it more concise . Meanwhile, the future study and the possible limitation of this method were also added (Lines 611-639). Therefore, we changed it as:

**" The TA model was used to decompose spatiotemporal SWC into time-stable patterns $M_{\hat{t}n}$, space-invariant temporal anomaly $A_{t\hat{n}}$, and space-variant temporal anomaly $R_{tn}$. This study indicated that underlying spatial patterns may exist in the $R_{tn}$ at small scales (e.g., small watersheds and hillslope) but may not at large scales such as the GENCAI network (~250 km²) in Italy. This was because the $R_{tn}$ at small scales was driven by "static" factors such as depth to the $CaCO_3$ layer and SOC at the Canadian site, while the $R_{tn}$ at large scales may be dominated by "dynamic" factors such as meteorological anomaly. Compared to the SA model, estimation of spatially distributed SWC was improved with the TA model at small watershed scales. This was because the TA model considered a fair amount of spatial variance in the $R_{tn}$, which was ignored in the SA model. Furthermore, the improved performance was observed mainly when soil water was drier or wetter than the average level, especially in drier conditions due to the high $\sigma_{\hat{n}}^2(R_{tn})$ value.**

**This study showed that outperformance of TA model over SA model is possible when $\sigma_{\hat{n}}^2(R_{tn})$ contributes substantial variance to the total variances of SWC, and significant spatial patterns (or EOFs) exist in the $R_{tn}$. Further application of the TA model for estimation of spatially distributed SWC at different scales and hydrological backgrounds is recommended. If the TA model parameters (i.e., $M_{\hat{t}n}$, EOF1 of the $R_{tn}$, and relationship between EC and $S_{t\hat{n}}$) are obtained from historical SWC dataset, a detailed spatially distributed SWC of near surface at watershed scales can be constructed from remote sensed SWC. Note that both models rely on previous SWC measurements for model parameters. Therefore, the future study should be directed to estimate spatially distributed SWC in un-gauged watersheds based on estimation of model parameters using pedotransfer functions. Since the TA model needs one more spatial parameter (i.e., $M_{\hat{t}n}$) than the SA model, advantage of the TA model may be weakened. Nevertheless, the TA model may be preferred if it estimates spatial SWC much better than the SA model such as at the dry conditions. The codes for decomposing SWC with the SA and TA models and**

**related EOF analysis were written in Matlab and are freely available from the authors upon request."**

I was furthermore wondering why S_tn from the Parry and Niemann (2007) based model are not also correlated against the site factors (i.e. soil properties, slope, etc., see table 1). This would help to understand the differences between the two investigated approaches.

Response:

For the Parry and Niemann (2007) based model (i.e., the SA) model, two components were included in the $S_{tn}$, i.e., spatial mean $S_{t\hat{n}}$ and spatial anomaly $Z_{tn}$. The $S_{tn}$ is the original soil water content. The spatial pattern of $S_{tn}$ varied with time, and its controlling factors have been extensively analyzed before. The temporal series of spatial mean $S_{t\hat{n}}$ cannot be correlated with site factors. So, we guess you mean the correlation between the underlying spatial pattern of $Z_{tn}$ and site factors.

Actually, we did correlate the underlying spatial pattern (i.e., EOF1) of $Z_{tn}$ from the Perry and Niemann (2007) to the site factors. However, the controls of EOF1 in $Z_{tn}$ were the same as those of $M_{\hat{t}n}$. This was because the spatial pattern of EOF1 in the $Z_{tn}$ was identical to the time-stable patterns $M_{\hat{t}n}$ in the TA model as also reflected by the correlation coefficient of 1 between EOF1 of $Z_{tn}$ and time-stable pattern $M_{\hat{t}n}$. Because of this reason, we did not show the correlation coefficients between EOF1 in the $Z_{tn}$ and site factors.

This has been explained at L3-6 of Page 6478 in previous copy " **Correlation analysis indicated that the spatial pattern of EOF1 in the $Z_{tn}$ was identical to the time-stable patterns $M_{\hat{t}n}$ in the TA model ($R$=1.0). The controls of EOF1 was therefore the same as those of $M_{\hat{t}n}$, and will be discussed later."**

Then a comment on section 2.3: does the performance of TA and SA not mainly depend on how well the respective ECs can be reproduced by the fitted function? I have the impression that the scatter in the S_tn – EC1 relationship is reduced for TA. . . *m*ay this be interpreted as such that the TA pre-filters more of the variance from the original data? But then, in a distant future, it may be desired to estimate the EOFs for ungauged catchments from a (future) database with data from water content observation networks, in a similar as done with pedotransfer functions.

However, in the case of the TA, one more spatial distribution would have to be estimated. This is certainly not an advantage. Could you comment on this?

Response:

(1) We agree with you that the goodness of fit for the relationship between EC1 and $S_{t\hat{n}}$ is also one factor influencing the performance of TA and SA. The percentages in amount of the variances in EC1 explained by the cosine function was a bit higher for the TA than the SA model. For example, $R^2$=0.76 at the near surface and 0.88 in the root zone for the TA model, while $R^2$=0.73 in both the near surface and root zone for the SA model. So, the reduced scatter in the EC1 and $S_{t\hat{n}}$ relationship in TA may also explain partly the outperformance of TA over SA. This was added at Lines 579-583:

**" The relationship between the $S_{t\hat{n}}$ and EC1 was better fitted by the cosine function in the TA model than the SA model (Figs. 4b and 6b), with $R^2$ of 0.76 versus 0.73 in the near surface and 0.88 versus 0.73 in the root zone. The reduced scatter in the $S_{t\hat{n}}$ and EC1 relationship in the TA model may also partly explain the outperformance of the TA model over the SA model."**

But we cannot conclude that the performance of the TA and the SA models MAINLY depend on how well the respective ECs can be reproduced by the fitted function. If this was the truth, the outperformance of TA over SA in the root zone should be more obviously than that in the near surface because the scatters for the two models were similar for the surface layer and the scatter of the TA model was much less than the SA model in the root zone. However, according to Fig.9, the outperformance of the TA model over the SA model was comparable between the near surface and root zone. Therefore, as we discussed in the discussion (Lines 584-593),

**" the outperformance of the TA model over the SA model depends on counterbalance among the variance of $R_{tn}$ explained in the TA model, the linear correlation between the $M_{\hat{t}n}$ and EOF1 of the $R_{tn}$, and the goodness of fit for the $S_{t\hat{n}}$ and EC1 relationship. For example, the variance of EOF1 in the $R_{tn}$ for the near surface (i.e., 264%$^2$) was much greater than that for the root zone (i.e., 43%$^2$). However, $M_{\hat{t}n}$ and underlying spatial patterns (EOF1) in the $R_{tn}$ in the root zone deviated more from a linear relationship, and**

**the reduced scatter in the $S_{t\hat{n}}$ and EC1 relationship in the TA model was more obviously in the root zone than in the near surface. As a result, the outperformance of the TA model was comparable between the near surface and root zone at the Canadian site (Fig. 9)."**

(2) We agree that the TA model is more complex than the SA model because one more spatial distribution has to be estimated. But on the other hand, estimation error is another factor that should be considered. Therefore, both model complexity and prediction errors should be taken into account during the model selection. This is why we introduced the AICc index to evaluate the two models. From the SWC data from the Canadian prairies, we found that when all 23 datasets were used and only EOF1 was considered, the TA model had lower AICc values than the SA model (please see L2-5 at Page 6481 in the previous copy). This indicated that even when penalty to complexity was given, the TA model was better than the SA model. Also considering that parameters in both models are estimated based on the same soil water content observation network, the TA model can be advantageous in case soil water distribution can be much better estimated.

However, as we added in the conclusions part (Lines 633-638): " **Therefore, the future study should be directed to estimate spatially distributed SWC in un-gauged watersheds based on estimation of model parameters using pedotransfer functions. Since the TA model needs one more spatial parameter (i.e., $M_{\hat{t}n}$) than the SA model, advantage of the TA model may be decreased. Nevertheless, the TA model may be preferred if it estimates spatial SWC much better than the SA model such as at the dry conditions."**

Finally, for the sake of clarity, I suggest to expand the sentence on P6472,L14-16 and convert it in a little section on how the site properties where compared to which model parameters. This section would nicely fit in before section 2.3. Also the multiple stepwise regressions used in table 1 should be mentioned here.
Otherwise I only have some specific comments. I recommend a publication of hessd-12-6467-2015 after revisions

Response:

The sentence " These properties were used to relate time-stable patterns and underlying spatial patterns of space-variant temporal anomaly to environmental factors." on P6472, L14-16 was removed. We mentioned all the properties we used for correlation analysis at Lines 147-152 as:

**" These properties included soil particle components (clay, silt, and sand contents), bulk density, soil organic carbon (SOC) content for the surface layer, A horizon depth, C horizon depth, depth to the $CaCO_3$ layer, leaf area index, elevation, cos(aspect), slope, curvature, gradient, upslope length, solar radiation, specific contributing area, convergence index, wetness index, and flow connectivity. Detailed information on the measurements can be found in Biswas et al. (2012)."**

We expanded this sentence in a paragraph immediately before section 2.3. The multiple stepwise regressions were also mentioned here. Therefore, we added a paragraph right before section 2.3 as (Lines 260-265):

**" The Pearson correlation coefficient (*R*) is used to explore the linear relationships between various spatial components in the two models (i.e., EOF1 of the $Z_{tn}$ in the SA model, $M_{\hat{t}n}$, and EOF1 of the $R_{tn}$ in the TA model) and environmental factors (i.e., soil, vegetative, and topographical properties). The multiple stepwise regressions are conducted to determined the percentage of variations in the spatial components that the controlling factors explain. "**

Specific comments P6468L4-6: this sentence disconnects the sentences before and after which belong together. It is difficult to understand what is meant. I would rephrase it.

Response:

We changed the first sentences (L2-9 at Page 6468) as (Lines 7-15):

**" A model was used to decompose spatiotemporal SWC into time-stable pattern (i.e, temporal mean), space-invariant temporal anomaly, and space-variant temporal anomaly. The space-variant temporal anomaly was further decomposed using the empirical orthogonal function for estimating spatially distributed SWC. This model was compared with a previous model that decomposes spatiotemporal SWC into spatial mean and spatial anomaly, with the latter being also decomposed using the EOF. These two models are termed temporal anomaly (TA) model and spatial anomaly (SA) model, respectively. "**

P6470L2 and L3: “may be further”?

Response:

Yes. we changed " be further" to "may be further" for both L2 and L3 on Page 6470.

Section 2.1.: I suggest presenting the study area in more detail and include soil textures, elevation differences and vegetation. It would be also nice to be informed about the CaCO2 layer before it is discussed in the material and methods.

Response:

We added more information on elevation differences, soil textures, and vegetation at Lines 127-129:

**" The elevation varies from 554.8 to 557.5 m. The soils are dominated by the clay loam textured Mollisols (Soil Survey Staff, 2010) and covered by mixed grass, i.e., smooth brome grass (*Bromus inermis*) and alfalfa (*Medicago sativa* L.)."**

The information on CaCO3 layer was also added at Lines 130-135:

**" Calcium carbonates ($CaCO_3$) derived mostly from fragments of limestone rocks are common in the Canadian Prairie. The $CaCO_3$ may be dissolved by the slightly acidic rainwater moving through the upper horizons but precipitate again in a lower horizon. The heterogeneous amount of infiltrated water resulted in a varying depth of $CaCO_3$ layer ranging from almost 0 m in the knolls to 2.1 m in the depressions."**

Section 2.2.: I found this section contains many long sentences, some of which are formulated in a misleading way.

Response:

We checked and revised this section to try to avoiding misunderstanding. This section was changed as (Lines 153-265) :

**"2.2 Statistical models for decomposing soil water content**

**Spatiotemporal SWC at small watershed scales was decomposed into three components: time-stable pattern, space-invariant temporal anomaly, and space-variant temporal anomaly. This model was compared with the one that decomposed SWC into spatial mean and spatial anomaly (Perry and Niemann, 2007). Both the space-variant temporal anomaly and spatial anomaly were decomposed using the EOF method. The two models are termed temporal anomaly (TA) model and spatial anomaly (SA) model,**

**respectively. Please refer to Fig. 1 for the differences of the two models. Each component will be explained in detail later. The explanation of nomenclatures is listed in Table A1. Because we focus on estimating spatial distribution of SWC at any given time, only spatial variances of SWC were taken into account. Therefore, the variance or covariance denotes the quantity in space without specifications.**

**2.2.1 The SA model**

**Perry and Niemann (2007) expressed SWC at location *n* and time *t*, $S_{tn}$, as (Fig. 1):**

$$S_{tn} = S_{t\hat{n}} + Z_{tn}, \qquad (1)$$

**where $S_{t\hat{n}}$ is the spatial mean SWC at time *t* (temporal forcing) and $Z_{tn}$ is the spatial anomaly of SWC (lumped spatial forcing and interactions). The subscript $\hat{n}$ ($\hat{t}$) indicates a space (time) averaged quantity.**

**According to Perry and Niemann (2007), $S_{t\hat{n}}$ can be estimated by remote sensing, water balance models, and in situ soil water measurement at a representative (or time-stable) location. The latter method was selected because the representative location can be easily determined with prior SWC datasets. By measuring SWC only at the most time-stable location *s* and future time *t*, $S_{ts}$, $S_{t\hat{n}}$ can be estimated using (Grayson and Western, 1998):**

$$S_{t\hat{n}} = \frac{S_{ts}}{1 + \delta_{\hat{ts}}}, \qquad (2)$$

**where the most time-stable location *s* was identified using time stability index of mean absolute bias error (Hu et al., 2010, 2012). The $\delta_{\hat{ts}}$ is the temporal mean relative difference of SWC at the most time-stable location *s* calculated with prior measurements.**

**Spatial anomaly $Z_{tn}$ can be reconstructed by the sum of the product of time-invariant spatial structures (EOFs) and the temporally varying coefficients (ECs) using the EOF method (Perry and Niemann, 2007; Joshi and Mohanty, 2010; Vanderlinden et al., 2012). The ECs correspond to the eigenvectors of the matrix of spatial covariance of the $Z_{tn}$, and the EOFs are obtained by projecting the $Z_{tn}$ onto the matrix ECs as: $\mathrm{EOFs} = Z_{tn}\,\mathrm{ECs}$. The number of EOF (or EC) series equals the number of sampling dates. Each EOF series corresponds to one value at each location, and each EC series has one value at each measurement time. Each EOF is chosen to be orthogonal to other EOFs, and the lower-**

order EOFs account for as much variance as possible. The sum of variances of all EOFs equals the sum of variances of $Z_{tn}$ from all measurement times.

Usually, a substantial amount of variance can be explained by a small number of EOFs. Johnson and Wichern (2002) suggested the eigenvalue confidence limits method for selecting the number of EOFs. Once the number of significant EOFs at a confidence level of 95% is selected, $Z_{tn}$ can be estimated as the sum of the product of significant EOFs and associated ECs as:

$$Z_{tn} = \sum \mathrm{EOF}^{sig} \times (\mathrm{EC}^{sig})^{T}, \qquad (3)$$

where $\mathrm{EOF}^{sig}$ represents the significant EOFs of the $Z_{tn}$ obtained during model development, $\mathrm{EC}^{sig}$ is the associated temporally varying coefficient, and the superscript *T* represents matrix transpose. Following Perry and Niemann (2007), the associated significant EC at time *t*, $\mathrm{EC}_t$ , is estimated by the cosine relationship between EC and $S_{t\hat{n}}$ developed using prior measurements:

$$\mathrm{EC}_t = a + b\cos\left(\frac{2\pi}{c} S_{t\hat{n}} - d\right), \qquad (4)$$

where *a*, *b*, *c*, and *d* are the fitted parameters using prior measurements and $S_{t\hat{n}}$ is estimated from Eq. (2). By using the continuous function, $\mathrm{EC}_t$ can be estimated at any $S_{t\hat{n}}$ values, which allows for the estimation of spatially distributed SWC at any soil water conditions.

### 2.2.2 The TA model

Mittelbach and Seneviratne (2012) decomposed the $S_{tn}$ into a time-stable pattern (i.e., temporal mean) and a temporal anomaly component (Fig. 1):

$$S_{tn} = M_{\hat{t}n} + A_{tn}, \qquad (5)$$

where $M_{\hat{t}n}$ is the time-stable pattern (spatial forcing) controlled by "static" factors such as soil properties and topography; $A_{tn}$ refers to the temporal anomaly (lumped temporal forcing and interactions). The variance of SWC, $\sigma^2_{\hat{n}}(S_{tn})$, is the sum of variance of the $M_{\hat{t}n}$,

$\sigma^2_{\hat{n}}(M_{\hat{t}n})$, variance of the $A_{tn}$, $\sigma^2_{\hat{n}}(A_{tn})$, and two times of covariance between $M_{\hat{t}n}$ and $A_{tn}$, $2\mathrm{cov}(M_{\hat{t}n}, A_{tn})$, which can be expressed as:

$$\sigma^2_{\hat{n}}(S_{tn}) = \sigma^2_{\hat{n}}(M_{\hat{t}n}) + 2\mathrm{cov}(M_{\hat{t}n}, A_{tn}) + \sigma^2_{\hat{n}}(A_{tn}). \qquad (6)$$

Because the $A_{tn}$ in Mittelbach and Seneviratne (2012) is a lumped term, it can be further decomposed into space-invariant temporal anomaly $A_{t\hat{n}}$ (temporal forcing) and space-variant temporal anomaly $R_{tn}$ (interactions) (Vanderlinden et al., 2012). At a watershed scale, the $A_{t\hat{n}}$ is controlled by temporally varying factors such as meteorological variables and vegetation. Positive and negative $A_{t\hat{n}}$ correspond to relatively wet and dry periods, respectively. The $R_{tn}$ refers to the redistribution of $A_{t\hat{n}}$ among different locations due to the interactions between spatial forcing and temporal forcing. For example, soil and topography regulate how much rainfall enters soil and how much water runs off or runs on at a location. This, in turn, dictates vegetation growth in a water-limited environment. Therefore, $S_{tn}$ can also be expressed as (Fig. 1):

$$S_{tn} = M_{\hat{t}n} + A_{t\hat{n}} + R_{tn}. \qquad (7)$$

The temporal trends of $A_{t\hat{n}}$ in Eq. (7) and $S_{t\hat{n}}$ in Eq. (1) are the same as both represent temporal forcing. Because the $A_{t\hat{n}}$ is space-invariant and orthogonal to the $M_{\hat{t}n}$ and $R_{tn}$ in a space, $\sigma^2_{\hat{n}}(S_{tn})$ in Eq. (6) can also be written as:

$$\sigma^2_{\hat{n}}(S_{tn}) = \sigma^2_{\hat{n}}(M_{\hat{t}n}) + 2\mathrm{cov}(M_{\hat{t}n}, R_{tn}) + \sigma^2_{\hat{n}}(R_{tn}), \qquad (8)$$

where $\mathrm{cov}(M_{\hat{t}n}, R_{tn})$ is the covariance between the $M_{\hat{t}n}$ and $R_{tn}$, and $\sigma^2_{\hat{n}}(R_{tn})$ is the variance of the $R_{tn}$. Apparently, $2\mathrm{cov}(M_{\hat{t}n}, R_{tn})$ equals $2\mathrm{cov}(M_{\hat{t}n}, A_{tn})$, and $\sigma^2_{\hat{n}}(R_{tn})$ equals $\sigma^2_{\hat{n}}(A_{tn})$. The percentage (%) contributions of $\sigma^2_{\hat{n}}(M_{\hat{t}n})$, $2\mathrm{cov}(M_{\hat{t}n}, R_{tn})$, and $\sigma^2_{\hat{n}}(R_{tn})$ to the $\sigma^2_{\hat{n}}(S_{tn})$ are calculated. The $\mathrm{cov}(M_{\hat{t}n}, R_{tn})$ can be negative at some conditions, for example, when the depressions correspond to greater $M_{\hat{t}n}$ and more negative $R_{tn}$ values in the discharge periods. This resulted in percentage contributions of $\sigma^2_{\hat{n}}(M_{\hat{t}n})$ and $\sigma^2_{\hat{n}}(R_{tn})$ > 100% and percentage contributions of $2\mathrm{cov}(M_{\hat{t}n}, R_{tn})$ < 0% (Mittelbach and Seneviratne, 2012;

**Brocca et al., 2014; Rötzer et al., 2015). If $R_{tn}$ is zero at any time or location, there are no interactions between spatial forcing and temporal forcing, $\sigma_{\hat{n}}^2(S_{tn})$ and the spatial trends of SWC are consistent over time. Therefore, $R_{tn}$ is directly responsible for temporal change in spatial variability of SWC.**

**If some underlying spatial patterns exist in $R_{tn}$, $R_{tn}$ can be reconstructed by the sum of the product of time-invariant spatial structures (EOFs) and time-dependent coefficients (ECs) using the EOF method. Note that the number of EOF (or EC) series also equals the number of sampling dates.**

**For estimation of spatially distributed SWC, $R_{tn}$ is estimated by the same method as $Z_{tn}$ using Eq. (3). The $M_{\hat{t}n}$ is estimated with prior measurements by:**

$$M_{\hat{t}n} = \frac{1}{m}\sum_{j=1}^{m} S_{tn}, \qquad (9)$$

**where $m$ is the number of previous measurement times, and $A_{t\hat{n}}$ is estimated by:**

$$A_{t\hat{n}} = S_{t\hat{n}} - M_{\hat{t}\hat{n}}, \qquad (10)$$

**where $M_{\hat{t}\hat{n}}$ is the spatial mean of $M_{\hat{t}n}$, and $S_{t\hat{n}}$ is estimated from SWC measurements at the most time-stable location using Eq. (2).**

**The Pearson correlation coefficient (*R*) is used to explore the linear relationships between various spatial components in the two models (i.e., EOF1 of the $Z_{tn}$ in the SA model, $M_{\hat{t}n}$, and EOF1 of the $R_{tn}$ in the TA model) and environmental factors (i.e., soil, vegetative, and topographical properties). The multiple stepwise regressions are conducted to determined the percentage of variations in the spatial components that the controlling factors explain."**

Equation (2): In this point the SA method deviates from the one described in Perry and Niemann (2009). Please point this out and explain and justify why you preferred to estimate S_tn in this way.

Response:

Actually, in the study of Perry and Niemann (2009), they did not estimate the mean soil water content but instead use the true value of mean soil water content for estimating soil water distribution. Meanwhile, they discussed how to estimate the mean soil water content. As we added in the revision (Lines 173-175):

**" According to Perry and Niemann (2007), $S_{t\hat{n}}$ can be estimated by remote sensing, water balance models, and in situ soil water measurement at a representative (or time-stable) location. "**

From Perry and Niemann (2009), we can find that they put more paragraphs on the discussion of the later (i.e., third) method. Therefore,

**" The latter method was selected because the representative location can be easily determined with prior SWC datasets. By measuring SWC only at the most time-stable location *s* and future time *t*, $S_{ts}$, $S_{t\hat{n}}$ can be estimated using (Grayson and Western, 1998):**

$$S_{t\hat{n}} = \frac{S_{ts}}{1+\delta_{\hat{ts}}}, \quad \textbf{(2)}$$

**where the most time-stable location *s* was identified using time stability index of mean absolute bias error (Hu et al., 2010, 2012). The $\delta_{\hat{ts}}$ is the temporal mean relative difference of SWC at the most time-stable location *s* calculated with prior measurements."** (Lines 175-183).

Different locations provide different accuracy of spatial average soil moisture. There are many indices which can be used to determine the best location. According to Hu et al. (2010, 2012), the mean absolute bias error is the best index to identify the most time-stable location for estimating the spatial average soil moisture. This is why we used Eq. (2) to estimate spatial average soil water content.

In summary, we used one of the methods that Perry and Niemann (2007) mentioned. As Perry and Niemann (2007) mentioned, the spatial average soil moisture for the near surface can also be estimated by the remote sensed SWC, and this is why we mentioned that **" If the TA model parameters (i.e., $M_{\hat{tn}}$, EOF1 of the $R_{tn}$, and relationship between EC and $S_{t\hat{n}}$) are obtained from historical SWC dataset, a detailed spatially distributed SWC of near surface at watershed scales can be constructed from remote sensed SWC."** (Lines 629-632). This also answered one comment made the Referee #2.

P6473L15-P6474L4: see remark on section 2.2. I only understood what was meant in this section after reading Perry and Niemann (2007). It is for example not clear from the text why the abbreviation of EC is used and that EC corresponds to the matrix of eigenvectors. The manuscript would gain considerably if this passage was better explained.

Response:

Please see the response about the comments on section 2.2.

We explained these paragraphs in more detail. Therefore, we revised these paragraphs as (Lines 184-194):

**" Spatial anomaly $Z_{tn}$ can be reconstructed by the sum of the product of time-invariant spatial structures (EOFs) and the temporally varying coefficients (ECs) using the EOF method (Perry and Niemann, 2007; Joshi and Mohanty, 2010; Vanderlinden et al., 2012). The ECs correspond to the eigenvectors of the matrix of spatial covariance of the $Z_{tn}$, and the EOFs are obtained by projecting the $Z_{tn}$ onto the matrix ECs as: $\mathrm{EOFs} = Z_{tn}\,\mathrm{ECs}$. The number of EOF (or EC) series equals the number of sampling dates. Each EOF series corresponds to one value at each location, and each EC series has one value at each measurement time. Each EOF is chosen to be orthogonal to other EOFs, and the lower-order EOFs account for as much variance as possible. The sum of variances of all EOFs equals the sum of variances of $Z_{tn}$ from all measurement times. "**

Equation (4): Please also explain shortly why it is necessary to approximate ECt by a continuous function

Response:

We approximate ETc with the cosine function for two reasons:

First, in the SA method, Perry and Niemann (2007) used the continuous function. We did the same thing for keeping consistency.

Second, by using the continuous function, $\mathrm{EC}_t$ can be estimated at any $S_{t\hat{n}}$ values, which allows for the estimation of spatially distributed SWC at any soil water conditions.

Therefore, we changed the related paragraph as (Lines 203-210):

**" Following Perry and Niemann (2007), the associated significant EC at time *t*, $\mathrm{EC}_t$ , is estimated by the cosine relationship between EC and $S_{t\hat{n}}$ developed using prior measurements:**

$$\mathrm{EC}_t = a + b\cos\left(\frac{2\pi}{c}S_{t\hat{n}} - d\right), \qquad \textbf{(4)}$$

**where *a*, *b*, *c*, and *d* are the fitted parameters using prior measurements and $S_{t\hat{n}}$ is estimated from Eq. (2). By using the continuous function, $EC_t$ can be estimated at any $S_{t\hat{n}}$ values, which allows for the estimation of spatially distributed SWC at any soil water conditions."**

P6479L8 and following: Percent of what? How can something contribute to another thing by more than 100%? What are %^2 (Figure 5)? It needs to be explained in the material and methods what "percents" is referring to.

Response:

We used the "%" as a unit for two quantity in this manuscript.

First, it was used to express the percent (%)of $\sigma^2_{\hat{n}}(M_{\hat{t}n})$, $2\mathrm{cov}(M_{\hat{t}n}, R_{tn})$, and $\sigma^2_{\hat{n}}(R_{tn})$ to the total variance of SWC, $\sigma^2_{\hat{n}}(S_{tn})$. So, it is the percent of the $\sigma^2_{\hat{n}}(S_{tn})$. We understand that it is weird to say something contribute to another thing by more than 100%. But as we added at Lines 240-245: " **The** $\mathrm{cov}(M_{\hat{t}n}, R_{tn})$ **can be negative at some conditions, for example, when the depressions correspond to greater** $M_{\hat{t}n}$ **and more negative** $R_{tn}$ **values in the discharge periods. This resulted in percentage contributions of** $\sigma^2_{\hat{n}}(M_{\hat{t}n})$ **and** $\sigma^2_{\hat{n}}(R_{tn})$ **> 100% and percentage contributions of** $2\mathrm{cov}(M_{\hat{t}n}, R_{tn})$ **< 0% (Mittelbach and Seneviratne, 2012; Brocca et al., 2014; Rötzer et al., 2015).**". Considering that previous studies on this topic used the same terminology, we just explained how these percentages can be more than 100% to avoid confusion.

Second, "**The SWC was measured on a volumetric basis and expressed as a percentage (%) volume of water per unit soil volume.**" (Lines 140-141).So the variance of soil water content should have the unit of $\%^2$.

P6479L18: arithmetic average?

Response:

Yes. we changed "average" to "arithmetic average".

P6481L19: These values do not fit to the y-axes of figure 7. Please adapt. Please also call out figure 8 already at this point.

Response:

Sorry, we made a mistake here, the value "4.05" should be "-4.05". We did not plot these data in Figure 7. In Figure 8, as we mentioned in the caption: " **At 0–0.2 m, negative Nash-Sutcliffe coefficient of efficiency values for three dates (22 October 2008, 27 August 2009, and 27 October 2009) are not shown**". This is done for better displaying the NSCE values for other dates.

P6483L2: Please be more specific with what you mean by "needed".

Response:

What we mean here is only EOF1 should be considered for estimating spatially distributed SWC because EOF2 and EOF3 contributed little to the SWC estimation. We changed the related sentence to:

" **Although three significant EOFs of the $R_{tn}$ existed in some cases, only EOF1 rather than higher-order EOFs of the $R_{tn}$ should be considered for the spatially distributed SWC estimation.**" (Lines 510-511).

.

***Interactive comment on*** **"Estimating spatially distributed soil water content at small watershed scales based on decomposition of temporal anomaly and time stability analysis"** ***by*** **W. Hu and B. C. Si**

**Anonymous Referee #2**

Received and published: 5 August 2015

**Overview**

The study describes a new approach (likely better "new concept") for investigating spatial-temporal variability of soil moisture at catchment scale. Specifically, the decomposition of spatiotemporal soil moisture patterns in three components was carried out: temporal mean, space-invariant temporal anomaly, and space-variant temporal anomaly. The new model (TA) was compared with the approach (SA) by *Perry and Niemann (2007)* who decomposed spatiotemporal soil moisture patterns into spatial mean and spatial anomaly. By using in situ observations from a transect in the Canadian Prairies, the authors obtained that TA model performs better than SA model, mainly in dry conditions in which the variability of the space-variant temporal anomaly is stronger.

**General Comments**

I found the paper well written, well-structured and clear. I also believe the topic is of interest for the readers of HESS as it describes a new concept for analysing spatiotemporal soil moisture patterns, based on new understanding of the different components driving soil moisture variability.

However, I believe that one aspect (method presentation) should be improved and I have two major comments to be addressed before the publication.

Response:

Thank you for reviewing our manuscript and your constructive comments. Please refer to all changes in the revised manuscript following our response.

*MINOR COMMENT*: The method is well-written, but still quite complex to be understood. By using a soil moisture dataset I have collected, I tried to visualize the different components in a 2D plot (see e.g., *Fig. 1*). Hoping to be correct, from the figure it's easier for me to understand how the SA and TA models work. I believe that this kind of visualization will facilitate the readers.

Response:

Thank you. We removed Fig.2 and 4 in the previous copy, and combine them in one figure (Fig. 3) as you suggested. Meanwhile, we put the meteorological data in Fig. 2 (see below).

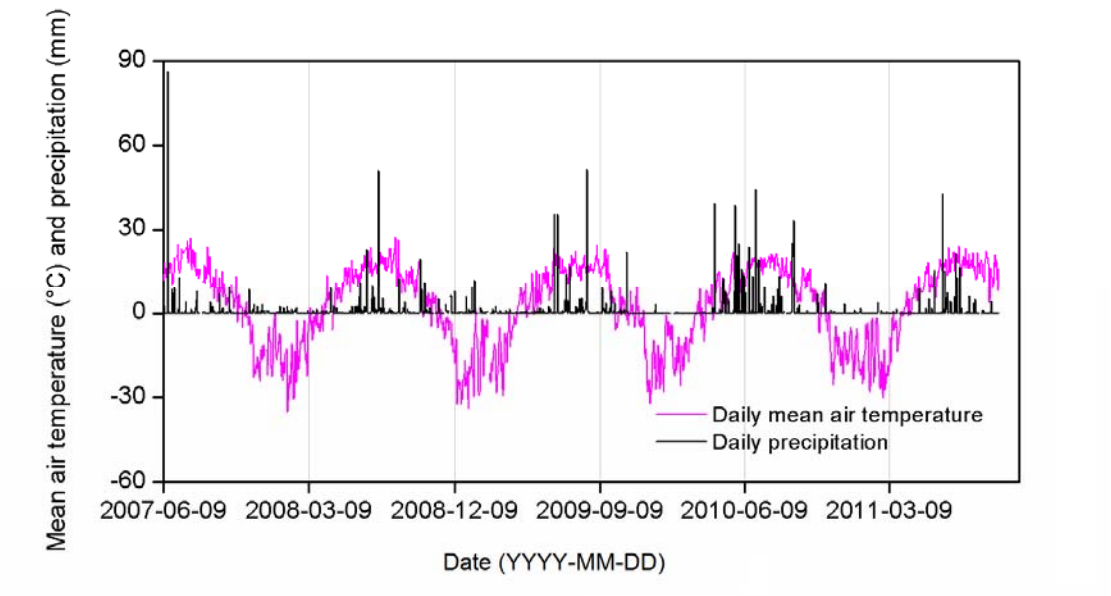


**Figure 2.** Daily mean air temperature and precipitation during the study period.

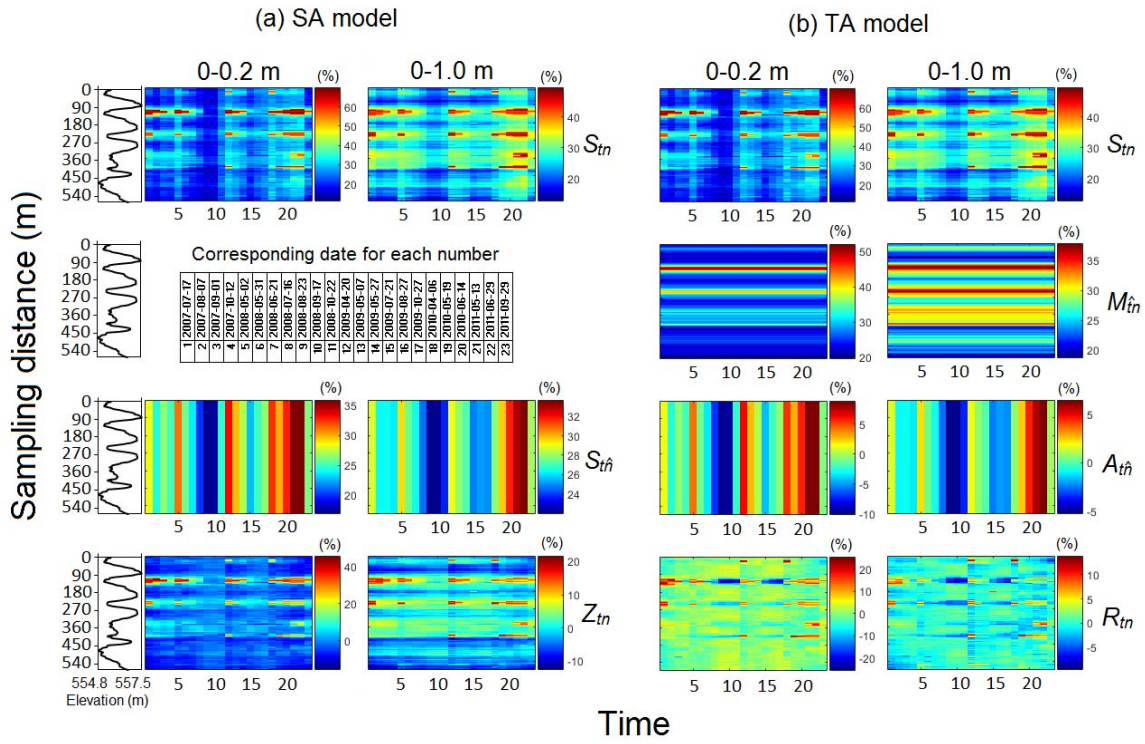


**Figure 3.** Components of soil water content in (a) the SA model (spatial mean soil water content $S_{t\hat{n}}$ and spatial anomaly $Z_{tn}$) and in (b) the TA model (time-stable pattern $M_{\hat{t}n}$, space-invariant

temporal anomaly $A_{t\hat{n}}$, and space-variant temporal anomaly $R_{tn}$) for 0–0.2 and 0–1.0 m. Also shown is the elevation.

*MAJOR COMMENT*: Only one study site is used to test the SA and TA models. Even though I am aware that the main purpose of the paper is the presentation of the "new concept" (TA model), I believe that the analysis for a different test site might be added. The dataset of the Canadian Prairies is quite famous (I have in mind at least 6 papers that makes use of this dataset), and the correlation between topographic and soil data with soil moisture for this dataset is well-know. I was wondering what could happens if a different dataset were employed (freely available or collected by the authors).

Response:

We added two other datasets, one from **A hillslope in the Chinese Loess Plateau (Hu et al., 2011), and one from the GENCAI network in Italy (**Brocca et al., 2012, 2013). Both datasets have been published and cited in this revision. The two datasets, respectively, represent a smaller and larger scale than the Canadian site. Our results indicate that the TA model outperformed the SA model at the Chinese site and they were identical at the Italian site (Please see the detailed results below). The outperformance of the TA model at small scales (Chinese site and Canadian site) can be attributed to the existence of underlying spatial patterns in the $R_{tn}$, while the absence of underlying spatial patterns in the $R_{tn}$ was the main reason why TA model was identical to that of the SA model at the Italian site. Similarly, because the first underlying spatial pattern (i.e., EOF1) explained greater percentages of the $\sigma^2_{\hat{n}}(R_{tn})$ at the Canadian site (44–61%) than the Chinese site (23%), the outperformance of the TA model over the SA model was more obvious at the former site (Fig. 9 and 10a). The related discussion was made in the Discussion section 4.2. By using the different datasets, it is easier to understand under which circumstance the TA model is preferable to the SA model for estimating spatially distributed SWC.

**" 3.3 Further application at other two sites with different scales**

**3.3.1 A hillslope in the Chinese Loess Plateau**

**Along a hillslope of 100 m in length in the Chinese Loess Plateau, SWC of 0–0.06 m was measured 136 times from 25 June 2007 to 30 August 2008 by a Delta-T Devices Theta probe (ML2x) at 51 locations (Hu et al., 2011). The hillslope was covered by *Stipa bungeana* Trin. and *Medicago sativa* L. in sandy loam and silt loam soils. On average, the**

$\sigma^2_{\hat{n}}(M_{\hat{tn}})$, $\sigma^2_{\hat{n}}(R_{tn})$, and $2\mathrm{cov}(M_{\hat{tn}}, R_{tn})$ contributed 53, 74 and -27% to the $\sigma^2_{\hat{n}}(S_{tn})$, indicating that both time-stable pattern and temporal anomalies were the main contributors to the $\sigma^2_{\hat{n}}(S_{tn})$. EOF analysis showed that only the EOF1 was statistically significant for both the $R_{tn}$ and $Z_{tn}$, and the EOF1 explained 23% and 47% of the total variances of $R_{tn}$ and $Z_{tn}$, respectively. This illustrated that underlying spatial patterns exist in the $R_{tn}$ on the hillslope. Cross validation was used to estimate the spatially distributed SWC along the hillslope. The results showed that the NSCE varied from -4.25 to 0.83 (TA model) and from -4.30 to 0.81 (SA model), with a mean value of 0.25 and 0.18, respectively. A paired samples T-test showed that the NSCE values for the TA model were significantly ($P$<0.05) greater than those for the SA model, indicating that the TA model outperformed the SA model. As Fig. 10a shows, the outperformance was greater when SWC deviated from intermediate conditions, especially for dry conditions, which was similar to the Canadian site.

### 3.3.2 The GENCAI network in Italy

In the GENCAI network (~250 km²) in Italy, SWC of 0–0.15 m was measured by a TDR probe at 46 locations at 34 times from February to December in 2009 (Brocca et al., 2012, 2013). The GENCAI area was dominated by grassland in flat topography with silty clay soils. The $\sigma^2_{\hat{n}}(M_{\hat{tn}})$, $\sigma^2_{\hat{n}}(R_{tn})$, and $2\mathrm{cov}(M_{\hat{tn}}, R_{tn})$ contributed 38, 68, and -7% to the $\sigma^2_{\hat{n}}(S_{tn})$ (Brocca et al., 2014), indicating the dominant contribution of temporal anomalies on SWC variability. The first three EOFs of the $R_{tn}$ explained 19, 16, and 8% of the total $\sigma^2_{\hat{n}}(R_{tn})$, and no EOFs were statistically significant, indicating no underlying spatial patterns exist in the $R_{tn}$. The EOF1 of the $Z_{tn}$ was significant and accounted for 37% of the variances in the $Z_{tn}$. Although the EOF1 of the $R_{tn}$ was not significant, it was considered in the TA model for estimating spatially distributed SWC. The cross validation indicate that the NSCE varied from -0.79 to 0.50 (TA model) and from -0.87 to 0.56 (SA model), with a mean value of 0.09 and 0.08, respectively. The SWC estimation based on these two models was not satisfactory except for a few days. As Fig. 10b shows, the differences in NSCE values between the two models were scattered around 0. A paired samples T-test showed that the NSCE values between the TA model and the SA model were

**not significant ($P$<0.05), indicating no differences in estimating spatially distributed SWC between these two models. "**

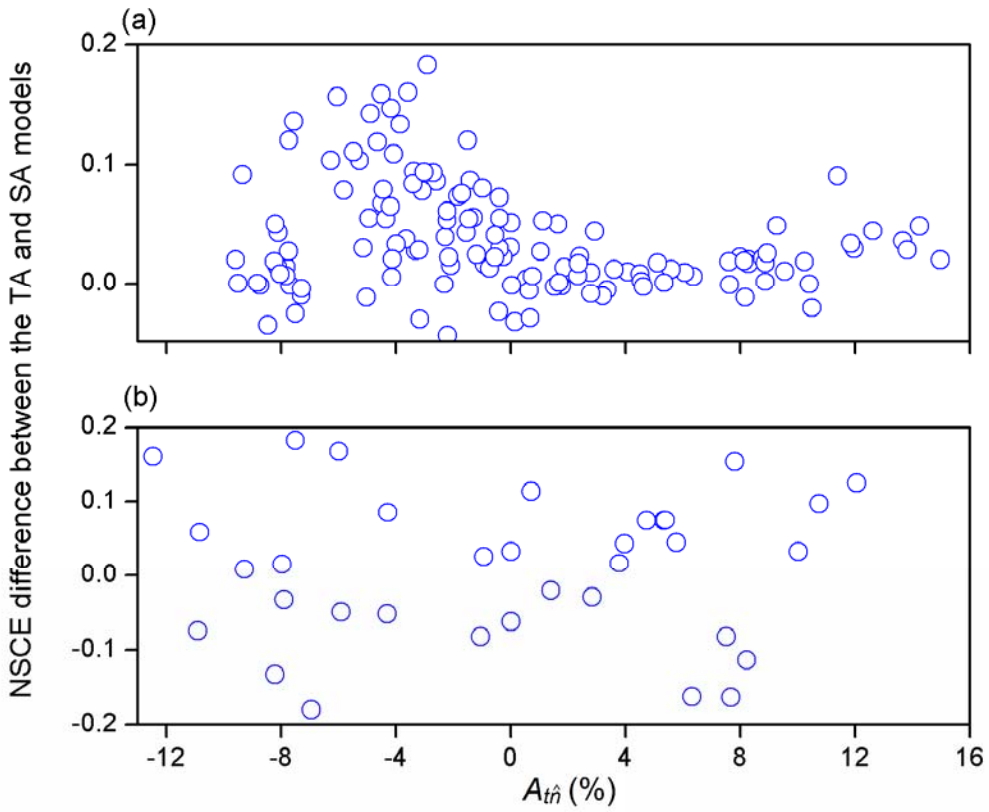


**Figure 10.** Difference between the Nash-Sutcliffe coefficient of efficiency (NSCE) of soil water content evaluation by the cross validation using the TA and SA models as a function of space-invariant temporal anomaly $A_{t\hat{n}}$ for (a) 0–0.06 m of the Chinese Loess Plateau hillslope and (b) 0–0.15 m of the GENCAI network in Italy.

*MAJOR COMMENT*: In the last sentence of the abstract it reads that "the TA model has potential to construct a spatially distributed SWC at watershed scales from remote sensed SWC." Even though it is potentially true, I believe that the paper makes only a first (short) step toward this interesting application. Indeed, for building the SA and TA models, the whole (spatially distributed) soil moisture dataset is used in the study.

Therefore, it was not demonstrated that TA (or SA) model provides good performance in reproducing spatial soil moisture pattern by using single measurements. At least, I suggest splitting the soil moisture dataset in a calibration and validation set. Otherwise, the models can be used only for understanding the different components driving soil moisture variability, not really as predictive tools (at least, it is not shown in the paper).

Response:

First, we have to classify that we did use the whole SWC dataset for building the TA and SA model in order to display the different components of these two models and determine their controls. But when we estimated the spatial SWC using the cross validation method, "**an iterative removal of 1 of the 23 dates is made for model development, and the SWC along the transect corresponding to the removed date is estimated iteratively.**" (Lines 273-275). From this aspect, we did evaluate the models in terms of reproducing spatial SWC by using independent measurements.

In this revision, we also used the external validation as you suggested for the main datasets (Canadian site). "**For the external validation, SWC from 14 dates of the first two years (from 17 July 2007 to 27 May 2009) is used for model development, and the SWC distribution of 9 dates in the second two years (from 21 July 2009 to 29 September 2011) is estimated.**" (Lines 275-278).

" **During the external validation, the TA model resulted in SWC estimation with NSCE values ranging from 0.61 to 0.85 near the surface and from 0.32 to 0.92 in the root zone except for two days (27 August 2009 and 27 October 2009 with NSCE of -2.63 and -5.12, respectively) at 0–0.2 m (Fig. 8). This suggested that the TA model performed well in estimating spatially distributed SWC patterns except on 27 August 2009 and 27 October 2009 at 0–0.2 m. The estimation in the root zone was also generally better than in the near surface.**" (Lines 442-448).

"**The difference in NSCE values between the TA and SA models for both validations are presented in Fig. 9. Generally, the difference decreased as $A_{t\hat{n}}$ increased, and then slightly increased with a further increase in $A_{t\hat{n}}$. A Paired Samples T-test indicated that the NSCE values of the TA model were significantly ($P<0.05$) greater than those of the SA model for both soil layers, irrespective of validation methods. This indicates that the TA model outperformed the SA model, particularly in dry conditions.**" (Lines 459-466).

Therefore, the external validation also supported the conclusion made by the cross validation. Because of this reason and for shortening the paragraph of this manuscript, we did not use external validation for the application of these two models to the other two sites.

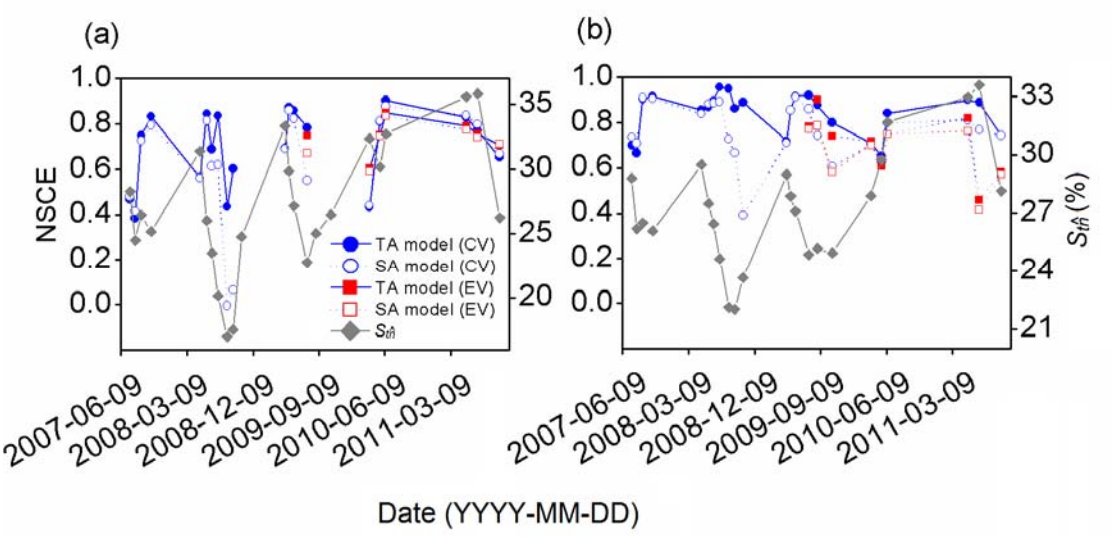


**Figure 8.** The Nash-Sutcliffe coefficient of efficiency (NSCE) of soil water content estimation using the TA and SA models for (a) 0–0.2 and (b) 0–1.0 m for both cross validation (CV) and external validation (EV). At 0–0.2 m, negative Nash-Sutcliffe coefficient of efficiency values for three dates (22 October 2008, 27 August 2009, and 27 October 2009) are not shown. Spatial mean soil water content $S_{t\hat{n}}$ on each measurement day is also shown.

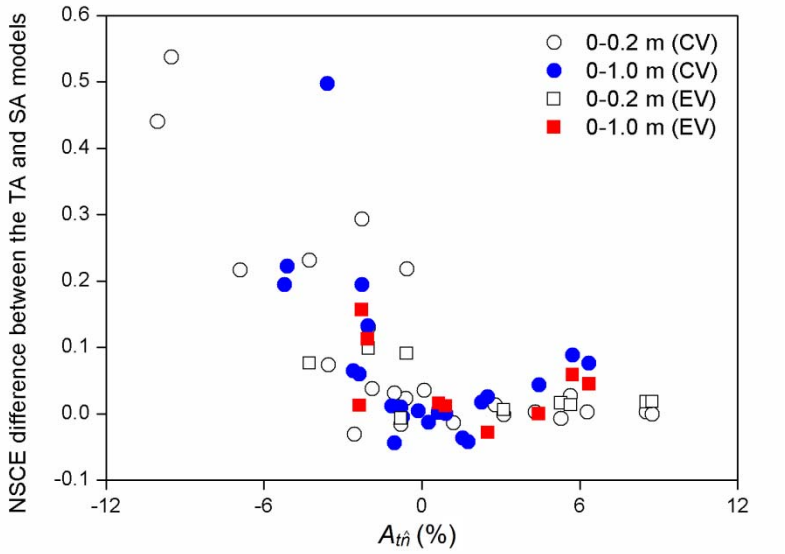


**Figure 9.** Difference between the Nash-Sutcliffe coefficient of efficiency (NSCE) of soil water content estimation by both cross validation (CV) and external validation (EV) using the TA and SA models as a function of space-invariant temporal anomaly $A_{t\hat{n}}$ for (a) 0–0.2 and (b) 0–1.0 m.

Moreover, it should be clarified how the authors believe to use the TA model to construct spatially distributed soil moisture from remote sensing observations.

Response:

As we answered above, spatial average SWC $S_{t\hat{n}}$ has to be estimated for estimating spatially distributed SWC**. " According to Perry and Niemann (2007),** $S_{t\hat{n}}$ **can be estimated by remote sensing, water balance models, and in situ soil water measurement at a representative (or time-stable) location.** ". In this manuscript, we used the later method to estimate the $S_{t\hat{n}}$**.**

As we revised the conclusion, **" If the TA model parameters (i.e.,** $M_{\hat{t}n}$**, EOF1 of the** $R_{tn}$**, and relationship between EC and** $S_{t\hat{n}}$**) are obtained from historical SWC dataset, a detailed spatially distributed SWC of near surface at watershed scales can be constructed from remote sensed SWC."** (Lines 629-632).

As mentioned by the first reviewer, some polishing of the text should be given (e.g., at page 6481, line 19 it reads NSCE of 4.05 and it should be -4.05) but it can be easily accomplished by the authors through a careful rereading of the manuscript.

Response:

Sorry for the mistake. We have changed 4.05 to -4.05.

We checked the manuscript carefully during this revision.

# Estimating spatially distributed soil water content at small watershed scales based on decomposition of temporal anomaly and time stability analysis

Wei Hu, Bing Cheng Si

*University of Saskatchewan, Department of Soil Science, Saskatoon, SK S7N 5A8, Canada*

## Abstract

Soil water content (SWC) at watershed scales is crucial to rainfall-runoff response. A model was used to decompose spatiotemporal SWC into time-stable pattern (i.e, temporal mean), space-invariant temporal anomaly, and space-variant temporal anomaly. The space-variant temporal anomaly was further decomposed using the empirical orthogonal function for estimating spatially distributed SWC. This model was compared with a previous model that decomposes spatiotemporal SWC into spatial mean and spatial anomaly, with the latter being also decomposed using the EOF. These two models are termed temporal anomaly (TA) model and spatial anomaly (SA) model, respectively. We aimed to test the hypothesis that underlying (i.e., time-invariant) spatial patterns exist in the space-variant temporal anomaly at the small watershed scale, and to examine the advantages of the TA model over the SA model in terms of estimation of spatially distributed SWC. For this purpose, a SWC dataset of near surface (0–0.2 m) and root zone (0–1.0 m) from a small watershed scale in the Canadian prairies was analyzed. Results showed that underlying spatial patterns exist in the space-variant temporal anomaly because of the permanent

controls of “static” factors such as depth to the $CaCO_3$ layer and organic carbon content. Combined with time stability analysis, the TA model improved estimation of spatially distributed SWC over the SA model, especially for dry conditions. Further application of these two models demonstrated an outperformance of the TA model at a hillslope in the Chinese Loess Plateau and an equivalent performance of these two models in the GENCAI network (~250 km²) in Italy. The TA model has potential to construct a spatially distributed SWC at small watershed scales from remote sensed SWC.

Keywords: Soil moisture; Soil water downscaling; Empirical orthogonal function; Statistical models; Time stability

## 1. Introduction

Soil water content (SWC) of surface soils exerts a major influence on a series of hydrological processes such as runoff and infiltration (Famiglietti et al., 1998; Vereecken et al., 2007; She et al., 2013a). Soil water content of the root zone is usually linked to vegetative growth (Wang et al., 2012; Ward et al., 2012; Jia and Shao, 2013). Accurate information on spatiotemporal SWC is a prerequisite for improving hydrological prediction and soil water management (Venkatesh et al., 2011; Champagne et al., 2012; She et al., 2013b; Zhao et al., 2013). While remote sensing has advanced SWC measurements of surface soils (<5 cm thick) at basin (2,500–25,000 $km^2$) and continental scales (Robinson et al., 2008), characterization of spatially distributed SWC at small watershed (0.1–80 $km^2$) scales still poses a

challenge. A method is needed for estimating spatially distributed SWC in the near surface and root zone at watershed scales.

Time stability of SWC, referring to similar spatial patterns of SWC across different measurement times (Vachaud et al., 1985; Brocca et al., 2009), has been used for estimating spatially distributed SWC (Starr, 2005; Perry and Niemann, 2007; Blöschl et al., 2009). This method is conceptually-appealing, but assumes completely time-stable spatial patterns of SWC.

The time-stable pattern does not explain all of the spatial variances in SWC, indicating the existence of time-variant components (Starr, 2005). In order to identify underlying patterns of SWC that have time-variant components, spatiotemporal SWC was decomposed into spatial mean and spatial anomaly, with the latter being further decomposed into the sum of the product of time-invariant spatial patterns (EOFs) and temporally varying but spatially constant coefficients (ECs) by the empirical orthogonal function (EOF) (Fig. 1) (Jawson and Niemann, 2007; Perry and Niemann, 2007, 2008; Joshi and Mohanty, 2010; Korres et al., 2010; Busch et al., 2012). Spatially distributed SWC estimates based on the decomposition of spatial anomaly outperformed those based on time-stable patterns (Perry and Niemann, 2007).

Recently, spatiotemporal SWC was also decomposed into temporal mean and temporal anomaly (Mittelbach and Seneviratne, 2012) (Fig. 1). Previous studies indicated that the contribution of temporal anomaly to the total spatial variance was notable (Mittelbach and Seneviratne, 2012; Brocca et al., 2014; Rötzer et al., 2015). These studies, however, only focused on surface soils and large scales (> 250 $km^2$).

65 Vanderlinden et al. (2012) suggested that the temporal mean may be further
66 decomposed into its spatial mean and residuals, and the temporal anomaly may be
67 further decomposed into space-invariant term (i.e., spatial mean of temporal anomaly)
68 and space-variant term (i.e., spatial residuals of temporal anomaly) (Fig. 1). Note that
69 the spatial variance in the temporal anomaly (Mittelbach and Seneviratne, 2012)
70 equals that in the space-variant term of temporal anomaly (Vanderlinden et al., 2012).
71 The further decomposition of temporal anomaly may be physically meaningful,
72 because the space-invariant and space-variant terms in the temporal anomaly may be
73 forced differently. However, the models of Mittelbach and Seneviratne (2012) and
74 Vanderlinden et al. (2012) have not been used for estimating spatially distributed
75 SWC. If the space-variant terms are ignored during the estimation of spatially
76 distributed SWC, their models are equivalent to that based on time-stable patterns.
77 Therefore, estimation of spatially distributed SWC may be improved by incorporating
78 the space-variant term of temporal anomaly if underlying (i.e., time-invariant) spatial
79 patterns exist in it.

80 To our knowledge, the importance of space-variant term of temporal anomaly and
81 its physical meaning at small watershed scales is not well-known. Based on previous
82 studies (Perry and Niemann, 2007; Mittelbach and Seneviratne, 2012; Vanderlinden et
83 al., 2012), we assume soil water dynamics at watershed scales can be decomposed
84 into three components (Fig. 1): (1) time-stable pattern (i.e., temporal mean, spatial
85 forcing): the "static" factors such as soil and topography control the pattern; (2)
86 space-invariant temporal anomaly (temporal forcing): the "dynamic" factors such as

meteorological variables and vegetation change with time, and therefore modify SWC in time, regardless of spatial locations; and (3) space-variant temporal anomaly (interactions between spatial forcing and temporal forcing): this term represents interactions between "static" and "dynamic" factors. For example, SWC recharge introduced by a rainfall may be modified by topography through runoff processes; SWC loss triggered by evapotranspiration may be regulated by topography through solar radiation exposure.

The "static" factors can be persistent in the space-variant temporal anomaly, and their impacts on the space-variant temporal anomaly likely change with time. Thus, we hypothesize that some underlying (i.e., time-invariant) spatial patterns exist in the space-variant temporal anomaly, and their impacts can be modulated by a time coefficient, both of which can be obtained by the EOF method (Fig. 1). If the hypothesis is true, estimation of spatially distributed SWC utilizing the EOF decomposition may outperform the one suggested by Perry and Niemann (2007). This is because: (1) the spatial anomaly which was decomposed using the EOF in Perry and Niemann (2007) lumped the time-stable pattern and space-variant temporal anomaly together (Fig. 1); (2) the underlying spatial patterns in the spatial anomaly may not fully capture both time-stable patterns and patterns in the space-variant temporal anomaly due to the possible nonlinear relations between these two terms.

Therefore, the objectives were (1) to test the hypothesis that underlying spatial patterns exist in the space-variant temporal anomaly at small watershed scales and (2) to examine whether the decomposition of space-variant temporal anomaly using the

EOF has any advantages over the decomposition of spatial anomaly (Perry and Niemann, 2007) for estimating spatially distributed SWC. Two steps were included in the estimation of spatially distributed SWC. First, spatial mean SWC was upscaled from SWC measurement at the most time-stable location using the time stability analysis. Then spatially distributed SWC was downscaled from the estimated spatial mean SWC. For this purpose, spatiotemporal SWC datasets from depths of near surface (0–0.2 m) and root zone (0–1.0 m) from a Canadian prairie landscape were used. Spatiotemporal SWC of 0–0.06 m from a hillslope (100 m) in the Chinese Loess Plateau and of 0–0.15 m from the GENCAI network (~250 km²) in Italy were also used to further demonstrate conditions under which the decomposition of spatial anomaly was beneficial to the estimation of spatially distributed SWC.

## 2. Materials and methods

### 2.1 Study area and data collection

The study area is located in St. Denis National Wildlife Area (52°12′ N, 106°50′ W) and has an area of 3.6 $km^2$ in the Canadian prairies. This area has a humid continental climate (Peel et al., 2007), with mean annual air temperature of 1.9 °C and mean annual precipitation of 402 mm during the study period (Fig. 2). A variety of depressions, knolls, and knobs result in a sequence of undulating slopes (Biswas et al., 2011). The elevation varies from 554.8 to 557.5 m. The soils are dominated by the clay loam textured Mollisols (Soil Survey Staff, 2010) and covered by mixed grass, i.e., smooth brome grass (*Bromus inermis*) and alfalfa (*Medicago sativa* L.). Near

surface soil porosity ranges from 38% (knolls) to 70% (depressions). Calcium carbonates ($CaCO_3$) derived mostly from fragments of limestone rocks are common in the Canadian Prairie. The $CaCO_3$ may be dissolved by the slightly acidic rainwater moving through the upper horizons but precipitate again in a lower horizon. The heterogeneous amount of infiltrated water resulted in a varying depth of $CaCO_3$ layer ranging from almost 0 m in the knolls to 2.1 m in the depressions. A sampling transect 576 m long with 128 sampling locations spaced at 4.5 m intervals was established over several rounded knolls and depressions. At each location, a time domain reflectometry probe was used to measure SWC of the near surface soil (0–0.2 m), and a neutron probe was used to collect SWC measurements at 0.2 m intervals between a depth of 0.2 and 1.0 m. The SWC was measured on a volumetric basis and expressed as a percentage (%) volume of water per unit soil volume. The SWC of the root zone was calculated by averaging the SWC of 0–0.2, 0.2–0.4, 0.4–0.6, 0.6–0.8, and 0.8–1.0 m. Soil water content was measured on 23 dates from 17 July 2007 to 29 September 2011. The SWC dataset, collected in all seasons except winter, accurately portrays the variations in soil water conditions in the study area. In addition to the SWC dataset, the soil, vegetative, and topographical properties were obtained at each sampling location. These properties included soil particle components (clay, silt, and sand contents), bulk density, soil organic carbon (SOC) content for the surface layer, A horizon depth, C horizon depth, depth to the $CaCO_3$ layer, leaf area index, elevation, cos(aspect), slope, curvature, gradient, upslope length, solar radiation, specific contributing area, convergence index, wetness index, and flow connectivity. Detailed

information on the measurements can be found in Biswas et al. (2012).

### 2.2 Statistical models for decomposing soil water content

Spatiotemporal SWC at small watershed scales was decomposed into three components: time-stable pattern, space-invariant temporal anomaly, and space-variant temporal anomaly. This model was compared with the one that decomposed SWC into spatial mean and spatial anomaly (Perry and Niemann, 2007). Both the space-variant temporal anomaly and spatial anomaly were decomposed using the EOF method. The two models are termed temporal anomaly (TA) model and spatial anomaly (SA) model, respectively. Please refer to Fig. 1 for the differences of the two models. Each component will be explained in detail later. The explanation of nomenclatures is listed in Table A1. Because we focus on estimating spatial distribution of SWC at any given time, only spatial variances of SWC were taken into account. Therefore, the variance or covariance denotes the quantity in space without specifications.

#### 2.2.1 The SA model

Perry and Niemann (2007) expressed SWC at location $n$ and time $t$, $S_{tn}$, as (Fig. 1):

$$S_{tn} = S_{t\hat{n}} + Z_{tn}, \qquad (1)$$

where $S_{t\hat{n}}$ is the spatial mean SWC at time $t$ (temporal forcing) and $Z_{tn}$ is the spatial anomaly of SWC (lumped spatial forcing and interactions). The subscript $\hat{n}$ ($\hat{t}$) indicates a space (time) averaged quantity.

According to Perry and Niemann (2007), $S_{t\hat{n}}$ can be estimated by remote sensing, water balance models, and in situ soil water measurement at a representative (or time-stable) location. The latter method was selected because the representative

location can be easily determined with prior SWC datasets. By measuring SWC only at the most time-stable location *s* and future time *t*, $S_{ts}$, $S_{t\hat{n}}$ can be estimated using (Grayson and Western, 1998):

$$S_{t\hat{n}} = \frac{S_{ts}}{1+\delta_{\hat{t}s}} \quad , \qquad (2)$$

where the most time-stable location *s* was identified using time stability index of mean absolute bias error (Hu et al., 2010, 2012). The $\delta_{\hat{t}s}$ is the temporal mean relative difference of SWC at the most time-stable location *s* calculated with prior measurements.

Spatial anomaly $Z_{tn}$ can be reconstructed by the sum of the product of time-invariant spatial structures (EOFs) and the temporally varying coefficients (ECs) using the EOF method (Perry and Niemann, 2007; Joshi and Mohanty, 2010; Vanderlinden et al., 2012). The ECs correspond to the eigenvectors of the matrix of spatial covariance of the $Z_{tn}$, and the EOFs are obtained by projecting the $Z_{tn}$ onto the matrix ECs as: $\mathrm{EOFs} = Z_{tn}\,\mathrm{ECs}$. The number of EOF (or EC) series equals the number of sampling dates. Each EOF series corresponds to one value at each location, and each EC series has one value at each measurement time. Each EOF is chosen to be orthogonal to other EOFs, and the lower-order EOFs account for as much variance as possible. The sum of variances of all EOFs equals the sum of variances of $Z_{tn}$ from all measurement times.

Usually, a substantial amount of variance can be explained by a small number of EOFs. Johnson and Wichern (2002) suggested the eigenvalue confidence limits method for selecting the number of EOFs. Once the number of significant EOFs at a

197 confidence level of 95% is selected, $Z_{tn}$ can be estimated as the sum of the product
198 of significant EOFs and associated ECs as:

199 $$Z_{tn} = \sum \mathrm{EOF}^{sig} \times (\mathrm{EC}^{sig})^{T}, \quad (3)$$

200 where $\mathrm{EOF}^{sig}$ represents the significant EOFs of the $Z_{tn}$ obtained during model
201 development, $\mathrm{EC}^{sig}$ is the associated temporally varying coefficient, and the
202 superscript *T* represents matrix transpose. Following Perry and Niemann (2007), the
203 associated significant EC at time *t*, $\mathrm{EC}_t$, is estimated by the cosine relationship
204 between EC and $S_{t\hat{n}}$ developed using prior measurements:

205 $$\mathrm{EC}_t = a + b\cos\left(\frac{2\pi}{c} S_{t\hat{n}} - d\right), \quad (4)$$

206 where *a*, *b*, *c*, and *d* are the fitted parameters using prior measurements and $S_{t\hat{n}}$ is
207 estimated from Eq. (2). By using the continuous function, $\mathrm{EC}_t$ can be estimated at
208 any $S_{t\hat{n}}$ values, which allows for the estimation of spatially distributed SWC at any
209 soil water conditions.

210 **2.2.2 The TA model**

211 Mittelbach and Seneviratne (2012) decomposed the $S_{tn}$ into a time-stable pattern
212 (i.e., temporal mean) and a temporal anomaly component (Fig. 1):

213 $$S_{tn} = M_{\hat{tn}} + A_{tn}, \quad (5)$$

214 where $M_{\hat{tn}}$ is the time-stable pattern (spatial forcing) controlled by "static" factors
215 such as soil properties and topography; $A_{tn}$ refers to the temporal anomaly (lumped
216 temporal forcing and interactions). The variance of SWC, $\sigma^2_{\hat{n}}(S_{tn})$, is the sum of
217 variance of the $M_{\hat{tn}}$, $\sigma^2_{\hat{n}}(M_{\hat{tn}})$, variance of the $A_{tn}$, $\sigma^2_{\hat{n}}(A_{tn})$, and two times of
218 covariance between $M_{\hat{tn}}$ and $A_{tn}$, $2\mathrm{cov}(M_{\hat{tn}}, A_{tn})$, which can be expressed as:

$$\sigma_{\hat{n}}^2\left(S_{tn}\right)=\sigma_{\hat{n}}^2\left(M_{\hat{t}n}\right)+2\mathrm{cov}(M_{\hat{t}n},A_{tn})+\sigma_{\hat{n}}^2\left(A_{tn}\right). \quad (6)$$

Because the $A_{tn}$ in Mittelbach and Seneviratne (2012) is a lumped term, it can be further decomposed into space-invariant temporal anomaly $A_{t\hat{n}}$ (temporal forcing) and space-variant temporal anomaly $R_{tn}$ (interactions) (Vanderlinden et al., 2012). At a watershed scale, the $A_{t\hat{n}}$ is controlled by temporally varying factors such as meteorological variables and vegetation. Positive and negative $A_{t\hat{n}}$ correspond to relatively wet and dry periods, respectively. The $R_{tn}$ refers to the redistribution of $A_{t\hat{n}}$ among different locations due to the interactions between spatial forcing and temporal forcing. For example, soil and topography regulate how much rainfall enters soil and how much water runs off or runs on at a location. This, in turn, dictates vegetation growth in a water-limited environment. Therefore, $S_{tn}$ can also be expressed as (Fig. 1):

$$S_{tn} = M_{\hat{t}n} + A_{t\hat{n}} + R_{tn}. \quad (7)$$

The temporal trends of $A_{t\hat{n}}$ in Eq. (7) and $S_{t\hat{n}}$ in Eq. (1) are the same as both represent temporal forcing. Because the $A_{t\hat{n}}$ is space-invariant and orthogonal to the $M_{\hat{t}n}$ and $R_{tn}$ in a space, $\sigma_{\hat{n}}^2\left(S_{tn}\right)$ in Eq. (6) can also be written as:

$$\sigma_{\hat{n}}^2\left(S_{tn}\right)=\sigma_{\hat{n}}^2\left(M_{\hat{t}n}\right)+2\mathrm{cov}(M_{\hat{t}n},R_{tn})+\sigma_{\hat{n}}^2\left(R_{tn}\right), \quad (8)$$

where $\mathrm{cov}(M_{\hat{t}n},R_{tn})$ is the covariance between the $M_{\hat{t}n}$ and $R_{tn}$, and $\sigma_{\hat{n}}^2\left(R_{tn}\right)$ is the variance of the $R_{tn}$. Apparently, $2\mathrm{cov}(M_{\hat{t}n},R_{tn})$ equals $2\mathrm{cov}(M_{\hat{t}n},A_{tn})$, and $\sigma_{\hat{n}}^2\left(R_{tn}\right)$ equals $\sigma_{\hat{n}}^2\left(A_{tn}\right)$. The percent (%) contributions of $\sigma_{\hat{n}}^2\left(M_{\hat{t}n}\right)$, $2\mathrm{cov}(M_{\hat{t}n},R_{tn})$, and $\sigma_{\hat{n}}^2\left(R_{tn}\right)$ to the $\sigma_{\hat{n}}^2\left(S_{tn}\right)$ are calculated. The $\mathrm{cov}(M_{\hat{t}n},R_{tn})$ can be negative at some conditions, for example, when the depressions correspond to

241 greater $M_{\hat{t}n}$ and more negative $R_{tn}$ values in the discharge periods. This resulted
242 in percentage contributions of $\sigma^2_{\hat{n}}\left(M_{\hat{t}n}\right)$ and $\sigma^2_{\hat{n}}\left(R_{tn}\right)$ > 100% and percentage
243 contributions of $2\mathrm{cov}(M_{\hat{t}n}, R_{tn})$ < 0% (Mittelbach and Seneviratne, 2012; Brocca et
244 al., 2014; Rötzer et al., 2015). If $R_{tn}$ is zero at any time or location, there are no
245 interactions between spatial forcing and temporal forcing, $\sigma^2_{\hat{n}}\left(S_{tn}\right)$ and the spatial
246 trends of SWC are consistent over time. Therefore, $R_{tn}$ is directly responsible for
247 temporal change in spatial variability of SWC.

248 If some underlying spatial patterns exist in $R_{tn}$, $R_{tn}$ can be reconstructed by the
249 sum of the product of time-invariant spatial structures (EOFs) and time-dependent
250 coefficients (ECs) using the EOF method. Note that the number of EOF (or EC) series
251 also equals the number of sampling dates.

252 For estimation of spatially distributed SWC, $R_{tn}$ is estimated by the same method
253 as $Z_{tn}$ using Eq. (3). The $M_{\hat{t}n}$ is estimated with prior measurements by:

254 $$M_{\hat{t}n} = \frac{1}{m}\sum_{j=1}^{m} S_{tn}, \qquad (9)$$

255 where $m$ is the number of previous measurement times, and $A_{t\hat{n}}$ is estimated by:

256 $$A_{t\hat{n}} = S_{t\hat{n}} - M_{\hat{t}\hat{n}}, \qquad (10)$$

257 where $M_{\hat{t}\hat{n}}$ is the spatial mean of $M_{\hat{t}n}$, and $S_{t\hat{n}}$ is estimated from SWC
258 measurements at the most time-stable location using Eq. (2).

259 The Pearson correlation coefficient ($R$) is used to explore the linear relationships
260 between various spatial components in the two models (i.e., EOF1 of the $Z_{tn}$ in the
261 SA model, $M_{\hat{t}n}$, and EOF1 of the $R_{tn}$ in the TA model) and environmental factors
262 (i.e., soil, vegetative, and topographical properties). The multiple stepwise regressions

are conducted to determined the percentage of variations in the spatial components that the controlling factors explain.

### 2.3 Validation and performance parameter

The TA model is more complicated than the SA model. In order to evaluate the two models for parsimony, AICc values are calculated (Burnham and Anderson, 2002) as:

$$\mathrm{AICc} = 2k + n\ln(RSS/n) + 2k(k+1)/(n-k-1), \qquad (11)$$

where $k$ is the number of parameters, $n$ is the sample size, and $RSS$ is the residual sum of squares.

Both cross validation and external validation are used to estimate SWC distribution with both models. For the cross validation, an iterative removal of 1 of the 23 dates is made for model development, and the SWC along the transect corresponding to the removed date is estimated iteratively. For the external validation, SWC from 14 dates of the first two years (from 17 July 2007 to 27 May 2009) is used for model development, and the SWC distribution of 9 dates in the second two years (from 21 July 2009 to 29 September 2011) is estimated.

The Nash-Sutcliffe coefficient of efficiency (NSCE) is used to evaluate the quality of estimation of spatially distributed SWC, which is expressed as:

$$\mathrm{NSCE} = 1 - \frac{\sigma_{\varepsilon}^2}{\sigma_{measure}^2}, \qquad (12)$$

where $\sigma_{measure}^2$ is the variance of measured SWC, and $\sigma_{\varepsilon}^2$ is the mean squared estimation error. A larger NSCE value implies a better quality of estimation. A paired samples T-test is used to test whether the NSCE values between the TA model and the SA model are statistically significant at $P<0.05$.

285 Many factors may affect the relative performance of spatially distributed SWC
286 estimation between the TA model and the SA model. First, the degree of
287 outperformance of the TA model over the SA model may depend on the amount of
288 $R_{tn}$ variance considered in the TA model. On one hand, the two models are identical
289 if variance of $R_{tn}$ is close to zero or there are negligible interactions between the
290 spatial and temporal components (Fig. 1). On the other hand, if no underlying spatial
291 patterns exist in the $R_{tn}$ or the underlying spatial patterns contributed little to the
292 total variance of the $R_{tn}$, the outperformance will be also very limited. Therefore, the
293 greater the variance of $R_{tn}$ can be considered in the TA model, the more likely the
294 TA model can outperform the SA model. Second, the way of EOF decomposition
295 may also affect the relative performance. In the SA model, EOF decomposition is
296 performed on lumped time-stable patterns $M_{\hat{t}n}$ and space-variant temporal anomaly
297 $R_{tn}$ (Perry and Niemann, 2007). In the TA model, however, EOF decomposition is
298 made only on $R_{tn}$. In theory, the two models will be identical if $M_{\hat{t}n}$ and the first
299 underlying spatial pattern (i.e., EOF1) of the $R_{tn}$ were perfectly correlated. If a
300 nonlinear relationship exists between them, lumping $M_{\hat{t}n}$ and $R_{tn}$ together, as in
301 the SA model, would weaken the model performance as compared to the TA model.
302 From this aspect, the greater deviation from a linear relationship between the $M_{\hat{t}n}$
303 and EOF1 of the $R_{tn}$, may lead to a greater outperformance of the TA model over the
304 SA model. Finally, the performances of both models rely on the estimation accuracy
305 of the $EC_t$ which depends on both goodness of fit of the cosine function (i.e., Eq. 4)
306 and estimation accuracy of the $S_{t\hat{n}}$. Because the same $S_{t\hat{n}}$ values are used for the

two models, the relative performance of the two models is related to the goodness of fit of Eq. (4).

# 3 Results

## 3.1 Components of SWC and their controls

### 3.1.1 Spatial mean $S_{t\hat{n}}$ and spatial anomaly $Z_{tn}$

The values of spatial mean $S_{t\hat{n}}$ in the SA model varied with seasons (Fig. 3a). In the spring, such as 2 May 2008 and 20 April 2009, snowmelt infiltration resulted in relatively great $S_{t\hat{n}}$ values. In the summer, however, even one month after large rainfall events (such as on 19 July 2008 and 21 June 2009), the high evapotranspiration by fast-growing vegetation resulted in small $S_{t\hat{n}}$. The values of $S_{t\hat{n}}$ also varied between inter-annual meteorological conditions. In 2008, there was less precipitation and higher air temperature than in 2010 (Fig. 2). As a result, $S_{t\hat{n}}$ was relatively smaller in 2008 than in 2010.

The spatial patterns of spatial anomaly $Z_{tn}$ were similar to those of original SWC patterns. The values of $Z_{tn}$ in wet periods (e.g., 13 May 2011) were much greater than in dry periods (e.g., 23 August 2008) in depressions (e.g., at a distance of 123 and 250 m); at other locations, however, the spatial anomaly was slightly less in wet periods than in dry periods for both soil layers. Moreover, the spatial anomaly in depressions was much greater in the near surface than in the root zone during the wet periods.

When SWCs of all 23 dates were used for model development, only EOF1 was

328 statistically significant (Fig. 4a), which accounted for 84.3% (0–0.2 m) and 86.5%
329 (0–1.0 m) of the variances in the $Z_{tn}$. Correlation analysis indicated that the spatial
330 pattern of EOF1 in the $Z_{tn}$ was identical to the time-stable patterns $M_{\hat{t}n}$ in the TA
331 model ($R$=1.0). The controls of EOF1 was therefore the same as those of $M_{\hat{t}n}$, and
332 will be discussed later. The relation between associated EC1 and $S_{t\hat{n}}$ can be fitted
333 well by the cosine function ($R^2$=0.73 at both the near surface and root zone) (Fig. 4b).

334 **3.1.2 Time-stable pattern $M_{\hat{t}n}$, space-invariant temporal anomaly $A_{t\hat{n}}$, and**
335 **space-variant temporal anomaly $R_{tn}$**

336 Figure 3b displays the three components in the TA model. The first component
337 $M_{\hat{t}n}$ fluctuated along the transect, with high values in depressions and low values on
338 knolls; $M_{\hat{t}n}$ also had greater spatial variability in the near surface (variance =36.7%$^2$)
339 than in the root zone (variance=19.5%$^2$). For both soil layers, SOC, depth to the
340 $CaCO_3$ layer, sand content, and wetness index are the dominant factors of $M_{\hat{t}n}$; they
341 together explained 74.5% (near surface ) and 75.6% (root zone) of the variances in the
342 $M_{\hat{t}n}$ (Table 1). In addition, the temporal trend of $A_{t\hat{n}}$ was the same as that of $S_{t\hat{n}}$
343 in the SA model (Fig. 3a) as both represent temporal forcing.

344 The $R_{tn}$ varied among landscape positions. At a sampling distance of 123 m (in a
345 depression), $R_{tn}$ was negative in dry periods such as 23 August 2008 and positive in
346 wet periods such as 13 May 2011. This was true for all depressions for both the near
347 surface and the root zone. Therefore, topographically lower positions usually
348 corresponded to more positive $R_{tn}$ during the wet periods and more negative $R_{tn}$
349 during the dry periods. This implies that topographically lower locations gained more

water during recharge and lost more water during discharge due to the interactions of spatial and temporal forcing. Furthermore, the absolute values of $R_{tn}$ were generally greater in the near surface than the root zone, indicating greater space-variant temporal anomaly for shallower depths.

The SWC variances and associated components (Eq. 8) also varied with time (Fig. 5). Often, wetter conditions corresponded to greater $\sigma^2_{\hat{n}}(S_{tn})$, as further indicated by moderate correlation between $\sigma^2_{\hat{n}}(S_{tn})$ and $S_{t\hat{n}}$ ($R^2$ of 0.51 and 0.38 for the near surface and the root zone, respectively). This was in agreement with others (Gómez-Plaza et al., 2001; Martínez-Fernández and Ceballos, 2003; Hu et al., 2011). Furthermore, there were greater $\sigma^2_{\hat{n}}(S_{tn})$ values at near surface than root zone, indicating greater variability of SWC in the near surface.

The time-invariant $\sigma^2_{\hat{n}}(M_{\hat{t}n})$ contributed to the $\sigma^2_{\hat{n}}(S_{tn})$ with percentages ranging from 25 to 795% for the near surface and from 40 to 174% for the root zone (Fig. 5). The $\sigma^2_{\hat{n}}(M_{\hat{t}n})$ exceeded the $\sigma^2_{\hat{n}}(S_{tn})$ mainly under dry conditions, such as July–October in 2008 and 2009. This excess was offset by the $\sigma^2_{\hat{n}}(S_{tn})$ and $2\mathrm{cov}(M_{\hat{t}n}, R_{tn})$, and the latter contributed negatively to the $\sigma^2_{\hat{n}}(S_{tn})$ with mean percentages of 210% for the near surface and 17% for the root zone. In the dry period, the negative contribution from $2\mathrm{cov}(M_{\hat{t}n}, R_{tn})$ was up to 1327% for the near surface and 122% for the root zone. These values are comparable to those in Mittelbach and Seneviratne (2012) and Brocca et al. (2014).

The $\sigma^2_{\hat{n}}(R_{tn})$ contributed less than other components (Fig. 5). The percentages of

371 $\sigma_{\hat{n}}^2(R_{tn})$ ranged from 11 to 632% (arithmetic average of 118%) for the near surface
372 and from 6 to 48% (arithmetic average of 19%) for the root zone; $\sigma_{\hat{n}}^2(R_{tn})$ tended to
373 contribute more in drier periods. This indicates that space-variant temporal anomaly
374 cannot be ignored, particularly in dry conditions. Furthermore, the contribution of
375 $\sigma_{\hat{n}}^2(R_{tn})$ was greater in the near surface than in the root zone, confirming stronger
376 temporal dynamics of soil water at the near surface. Compared with larger scale
377 studies (Mittelbach and Seneviratne, 2012; Brocca et al., 2014), $\sigma_{\hat{n}}^2(R_{tn})$ of the near
378 surface in this study contributed more to $\sigma_{\hat{n}}^2(S_{tn})$, with a mean percentage
379 contribution of 118%, versus 9–68% in other studies (Mittelbach and Seneviratne,
380 2012; Brocca et al., 2014). This indicates that interactions between spatial and
381 temporal forcing were stronger, resulting in relatively more intensive temporal
382 dynamics of soil water in our study area than at larger scales.

383 Three significant EOFs of $R_{tn}$ for both soil layers were identified when SWC of
384 all 23 dates were used for model development. The first three EOFs explained 61.1,
385 13.4, and 8.1% respectively, of the total $R_{tn}$ variance for the near surface, and 44.3,
386 20.2, and 12.4%, respectively, of the total $R_{tn}$ variance for the root zone. Therefore,
387 our hypothesis that underlying spatial patterns exist in the $R_{tn}$ was accepted. Due to
388 the negligible contribution of EOF2 and EOF3 to the estimation of spatially
389 distributed SWC, only EOF1 is shown in Fig. 6a. The associated EC1 changed with
390 soil water conditions ($S_{t\hat{n}}$) (Fig. 6b). When SWC was close to average levels, the EC1
391 was close to 0, resulting in negligible $R_{tn}$. This was in accordance with Mittelbach
392 and Seneviratne (2012) and Brocca et al. (2014), who showed that the spatial variance

of temporal anomaly was the smallest when water contents were close to average levels. The cosine function (Eq. 4) explained a large amount of the variances in EC1 for both soil layers ($R^2$=0.76 at the near surface and 0.88 in the root zone).

The contribution of EOF1 to the space-variant temporal anomaly can be examined through the product of the EOF1 and the associated EC1. EC1 values tended to be positive during wet periods and negative during dry periods (Fig. 6b); more positive EOF1 values were usually observed at locations with greater $M_{\hat{t}n}$ values (Figs. 3b and 6a). Therefore, the product of EOF1 and EC1 led to greater temporal SWC dynamics at wetter locations of both layers in both the wet and dry periods.

Depth to the $CaCO_3$ layer and SOC had significant, positive correlations with EOF1 for both soil layers ($R$ ranging from 0.76 to 0.88; Table 1). They jointly accounted for 81.6% (near surface) and 81.0% (root zone) of the variances in EOF1. This implies that locations with a greater depth to the $CaCO_3$ layer and SOC, which correspond to wetter locations such as depressions, usually have greater temporal SWC dynamics during both wet and dry periods.

### 3.2 Estimation of spatially distributed SWC

When all 23 datasets were used and only EOF1 was considered, the TA model had an AICc value of 4093 for the near surface and 562 for the root zone, while the corresponding values for the SA model were 6370 and 3460. This indicated that even when penalty to complexity was given, the TA model was better than the SA model. The two models in terms of spatially distributed SWC estimation are compared below.

#### 3.2.1 The TA model

415 The $R_{tn}$ terms and associated EOFs differed slightly with each validation. The
416 number of significant EOFs varied between one (accounting for 60% of the total cases)
417 and three for both soil layers. A paired samples T-test indicated that more EOFs did
418 not result in a significant increase of NSCE in the estimation of spatially distributed
419 SWC for both validation methods, because AICc values increased greatly with the
420 increasing number of parameters resulting from more EOFs (data not shown). This
421 indicates that higher-order EOFs, even if they are statistically significant, are
422 negligible for SWC prediction. Therefore, SWC distribution was estimated with
423 EOF1 only.

424 Estimated SWCs generally approximated those measured at different soil water
425 conditions during the cross validation (Fig. 7). However, on 27 October 2009, there
426 were unsatisfactory estimates at the 100–140 and 220–225 m locations near the
427 surface. Unsatisfactory NSCE values of -4.05, -1.83, and -3.81 were obtained in the
428 near surface in only three of the 23 dates, which were all in the fall (22 October 2008,
429 27 August 2009, and 27 October 2009, respectively). The poor performance obtained
430 with the TA model on those dates was a result of overestimation in depressions, where
431 strong evapotranspiration and deep drainage resulted in much lower SWC than in the
432 spring. These dates also corresponded to a high percentage of contribution of
433 $\sigma_{\hat{n}}^2(R_{tn})$ to the $\sigma_{\hat{n}}^2(S_{tn})$ (203–439%). For August 23 and September 17 in 2008,
434 which were in dry periods, $\sigma_{\hat{n}}^2(R_{tn})$ of the near surface also contributed highly to the
435 $\sigma_{\hat{n}}^2(S_{tn})$ (580 and 630%). Because a fair amount of $\sigma_{\hat{n}}^2(R_{tn})$ was accounted for
436 with the TA model, the TA model performed satisfactorily (NSCE of 0.43 and 0.60).

437 For the remaining 20 dates, the resulting NSCE value ranged from 0.38 to 0.90 in the
438 near surface and from 0.65 to 0.96 in the root zone (Fig. 8). This suggests that the TA
439 model was generally satisfactory, with better performance in the root zone than in the
440 near surface.

441 During the external validation, the TA model resulted in SWC estimation with
442 NSCE values ranging from 0.61 to 0.85 near the surface and from 0.32 to 0.92 in the
443 root zone except for two days (27 August 2009 and 27 October 2009 with NSCE of
444 -2.63 and -5.12, respectively) at 0–0.2 m (Fig. 8). This suggested that the TA model
445 performed well in estimating spatially distributed SWC patterns except on 27 August
446 2009 and 27 October 2009 at 0–0.2 m. The estimation in the root zone was also
447 generally better than in the near surface.

448 **3.2.2 Comparison with the SA model**

449 One significant EOF of $Z_{tn}$ was identified for both soil layers, irrespective of the
450 validation method. The SA model with only EOF1 produced reasonable SWC
451 estimations for both validations in all dates in the root zone and in every date except
452 five dates (23 August 2008, 17 September 2008, 22 October 2008, 27 August 2009,
453 and 27 October 2009) in the near surface (Fig. 8). Similarly, when more EOFs were
454 included, NSCE values did not increase significantly (data not shown) and
455 consequently, estimation of spatially distributed SWC was not improved. This was
456 because EOF2 and EOF3 together explained a very limited (<10%) amount of
457 variability of $Z_{tn}$ and thus had low predictive power in terms of variance.

458 The difference in NSCE values between the TA and SA models for both validations

459 are presented in Fig. 9. Generally, the difference decreased as $A_{t\hat{n}}$ increased, and
460 then slightly increased with a further increase in $A_{t\hat{n}}$. A paired samples T-test
461 indicated that the NSCE values of the TA model were significantly ($P$<0.05) greater
462 than those of the SA model for both soil layers, irrespective of validation methods.
463 This indicates that the TA model outperformed the SA model, particularly in dry
464 conditions. This was because when soil was dry, there was a high contribution of
465 $\sigma_{\hat{n}}^2(R_{tn})$, and thus strong variability in the space-variant temporal anomaly.

466 **3.3 Further application at other two sites with different scales**

467 **3.3.1 A hillslope in the Chinese Loess Plateau**

468 Along a hillslope of 100 m in length in the Chinese Loess Plateau, SWC of 0–0.06
469 m was measured 136 times from 25 June 2007 to 30 August 2008 by a Delta-T
470 Devices Theta probe (ML2x) at 51 locations (Hu et al., 2011). The hillslope was
471 covered by *Stipa bungeana* Trin. and *Medicago sativa* L. in sandy loam and silt loam
472 soils. On average, the $\sigma_{\hat{n}}^2(M_{\hat{t}n}), \sigma_{\hat{n}}^2(R_{tn})$, and $2\mathrm{cov}(M_{\hat{t}n}, R_{tn})$ contributed 53, 74
473 and -27% to the $\sigma_{\hat{n}}^2(S_{tn})$, indicating that both time-stable pattern and temporal
474 anomalies were the main contributors to the $\sigma_{\hat{n}}^2(S_{tn})$. EOF analysis showed that only
475 the EOF1 was statistically significant for both the $R_{tn}$ and $Z_{tn}$, and the EOF1
476 explained 23% and 47% of the total variances of $R_{tn}$ and $Z_{tn}$, respectively. This
477 illustrated that underlying spatial patterns exist in the $R_{tn}$ on the hillslope. Cross
478 validation was used to estimate the spatially distributed SWC along the hillslope. The
479 results showed that the NSCE varied from -4.25 to 0.83 (TA model) and from -4.30 to
480 0.81 (SA model), with a mean value of 0.25 and 0.18, respectively. A paired samples

T-test showed that the NSCE values for the TA model were significantly ($P$<0.05) greater than those for the SA model, indicating that the TA model outperformed the SA model. As Fig. 10a shows, the outperformance was greater when SWC deviated from intermediate conditions, especially for dry conditions, which was similar to the Canadian site.

### 3.3.2 The GENCAI network in Italy

In the GENCAI network (~250 km²) in Italy, SWC of 0–0.15 m was measured by a TDR probe at 46 locations at 34 times from February to December in 2009 (Brocca et al., 2012, 2013). The GENCAI area was dominated by grassland in flat topography with silty clay soils. The $\sigma_{\hat{n}}^2\left(M_{\hat{tn}}\right)$, $\sigma_{\hat{n}}^2\left(R_{tn}\right)$, and $2\mathrm{cov}(M_{\hat{tn}},R_{tn})$ contributed 38, 68, and -7% to the $\sigma_{\hat{n}}^2\left(S_{tn}\right)$ (Brocca et al., 2014), indicating the dominant contribution of temporal anomalies on SWC variability. The first three EOFs of the $R_{tn}$ explained 19, 16, and 8% of the total $\sigma_{\hat{n}}^2\left(R_{tn}\right)$, and no EOFs were statistically significant, indicating no underlying spatial patterns exist in the $R_{tn}$. The EOF1 of the $Z_{tn}$ was significant and accounted for 37% of the variances in the $Z_{tn}$. Although the EOF1 of the $R_{tn}$ was not significant, it was considered in the TA model for estimating spatially distributed SWC. The cross validation indicate that the NSCE varied from -0.79 to 0.50 (TA model) and from -0.87 to 0.56 (SA model), with a mean value of 0.09 and 0.08, respectively. The SWC estimation based on these two models was not satisfactory except for a few days. As Fig. 10b shows, the differences in NSCE values between the two models were scattered around 0. A paired samples T-test showed that the NSCE values between the TA model and the SA model were

not significant ($P$<0.05), indicating no differences in estimating spatially distributed SWC between these two models.

# 4 Discussion

## 4.1 Controls of the $M_{\hat{tn}}$ and $R_{tn}$

The $R_{tn}$ played an important role in the temporal change of spatial patterns in SWC. The underlying spatial patterns and physical meaning in the $R_{tn}$ were examined in our study for the first time. Although three significant EOFs of the $R_{tn}$ existed in some cases, only EOF1 rather than higher-order EOFs of the $R_{tn}$ should be considered for the spatially distributed SWC estimation. Among many factors influencing the EOF1 of the $R_{tn}$, depth to the $CaCO_3$ layer followed by the SOC, were the most important factors. Depressions have deeper $CaCO_3$ layers than knolls, and the shallow $CaCO_3$ layer on knolls limited water infiltration during rainfall or snowmelt, resulting in less water recharge on knolls than in depressions. The depth to $CaCO_3$ layer and SOC were negatively correlated with elevation ($R$=-0.54, $P$<0.01). Therefore, the influence of depth to $CaCO_3$ layer and SOC partially reflected the role of topography in driving snowmelt runoff along slopes in the spring, which contributes to increasing water recharge in depressions. Locations with greater SOC usually corresponded to vegetation with a larger leaf area index ($R$=0.23, $P$<0.05), which would also result in higher evapotranspiration and more water loss during discharge periods.

As Table 1 shows, both the depth to the $CaCO_3$ layer and SOC controlled the $M_{\hat{tn}}$.

This was because deeper $CaCO_3$ layers and higher SOC were observed in depressions where soils were usually wetter in most of the year because of the snowmelt runoff in the spring and rainfall runoff in the summer and autumn (van der Kamp et al., 2003). Therefore, the roles of soil and topography were two-fold: On one hand, they were highly correlated with the time-stable patterns and thus time stability of SWC (Gómez-Plaza et al., 2000; Mohanty and Skaggs, 2001; Grant et al., 2004); On the other hand, they, interplaying with temporal forcing, triggered local-specific soil water change and destroyed time stability of SWC. Their roles in protecting time stability persisted, but their roles in destroying time stability varied with time. Greater $\sigma_{\hat{n}}^2(R_{tn})$ implies greater contribution of these factors in soil water dynamics, resulting in less time stability of SWC.

### 4.2 Model performance for spatially distributed SWC estimation

The outperformance of the TA model for estimating spatial SWC at the Canadian site and Chinese site can be partly explained by the high contribution percentages (average of 19–118%) of the $\sigma_{\hat{n}}^2(R_{tn})$ to the total variance. When SWC is close to average levels, $R_{tn}$ is also close to zero, resulting in negligible variance contribution from $R_{tn}$ to the total variance. In this case, the soil water patterns are stable, the SA model performs well, and there will be little differences between these two models. As is well known, the spatial patterns in soil water contents are inherently time unstable. For example, when evapotranspiration becomes the dominant process at the small watershed scale, more water will be lost in depressions due to the denser vegetation than on knolls (Millar, 1971; Biswas et al., 2012), effectively diminishing

546 the spatial patterns and increasing temporal instability. In this case, the $\sigma_{\hat{n}}^2(R_{tn})$
547 contributes more to the total variance (e.g., high up to 632%) and the TA model may
548 outperform the SA model. This explained why the outperformance of TA model was
549 more obvious in the dry conditions. For the GENCAI network in Italy, although the
550 $\sigma_{\hat{n}}^2(R_{tn})$ contributed 68% of the total variance, the performance of the TA model was
551 identical to the SA model. This was because there were no underlying spatial patterns
552 in the $R_{tn}$. Similarly, because the first underlying spatial pattern (i.e., EOF1)
553 explained greater percentages of the $\sigma_{\hat{n}}^2(R_{tn})$ at the Canadian site (44–61%) than the
554 Chinese site (23%), the outperformance of the TA model over the SA model was more
555 obvious at the former site (Fig. 9 and 10a). Therefore, the TA model is advantageous
556 only if the contribution of $\sigma_{\hat{n}}^2(R_{tn})$ to the total variance is substantial and underlying
557 spatial patterns exist in the $R_{tn}$.

558 The existence of underlying spatial patterns in the $R_{tn}$ is related to the controlling
559 factors, which may be scale-specific. At small scales, "static" factors such as the depth
560 to the $CaCO_3$ layer and SOC at the Canadian site may affect not only the time-stable
561 patterns but also the $R_{tn}$. The persistent influence of "static" factors on the $R_{tn}$
562 resulted in significant underlying spatial patterns in the $R_{tn}$. Thus, the TA model
563 outperformed the SA model at the small scales. At large scales such as basin scale or
564 greater, time-stable patterns may be controlled by, in addition to soil and topography
565 (Mittelbach and Seneviratne, 2012), the climate gradient (Sherratt and Wheater, 1984);
566 at those scales, $R_{tn}$ is more likely to be controlled by the meteorological anomaly
567 (i.e., spatially random variation) (Walsh and Mostek, 1980), and the effects of soil and

topography may be reduced. Consequently, spatial patterns in the $R_{tn}$ may be weakened and the TA model may have no advantages over the SA model such as for the Italian site.

The $M_{\hat{tn}}$ and the underlying spatial patterns (EOF1) in the $R_{tn}$ were controlled by the same spatial forcing (e.g., depth to $CaCO_3$ layer and SOC) at the Canadian site (Table 1), and they were correlated with an $R^2$ of 0.83 for the near surface and 0.42 for the root zone. Although the relationships between $M_{\hat{tn}}$ and $R_{tn}$ were strong, they were not strictly linear, suggesting that $M_{\hat{tn}}$ and $R_{tn}$ were affected differently by these factors. Therefore, the nonlinear relationship between $M_{\hat{tn}}$ and $R_{tn}$ partially contributed to the outperformance of the TA model over the SA model.

The relationship between the $S_{t\hat{n}}$ and EC1 was better fitted by the cosine function in the TA model than the SA model (Figs. 4b and 6b), with $R^2$ of 0.76 versus 0.73 in the near surface and 0.88 versus 0.73 in the root zone. The reduced scatter in the $S_{t\hat{n}}$ and EC1 relationship in the TA model may also partly explain the outperformance of the TA model over the SA model.

Therefore, the outperformance of the TA model over the SA model depends on counterbalance among the variance of $R_{tn}$ explained in the TA model, the linear correlation between the $M_{\hat{tn}}$ and EOF1 of the $R_{tn}$, and the goodness of fit for the $S_{t\hat{n}}$ and EC1 relationship. For example, the variance of EOF1 in the $R_{tn}$ for the near surface (i.e., $264\%^2$) was much greater than that for the root zone (i.e., $43\%^2$). However, $M_{\hat{tn}}$ and underlying spatial patterns (EOF1) in the $R_{tn}$ in the root zone deviated more from a linear relationship, and the reduced scatter in the $S_{t\hat{n}}$ and EC1

590 relationship in the TA model was more obviously in the root zone than in the near
591 surface. As a result, the outperformance of the TA model was comparable between the
592 near surface and root zone at the Canadian site (Fig. 9).

593 In the real world, the relations between the $M_{\hat{tn}}$ and underlying spatial patterns in
594 the $R_{tn}$ may rarely be perfectly linear. Therefore, when underlying spatial patterns
595 exist in the $R_{tn}$ and the $R_{tn}$ has substantial variances, the TA model is preferable to
596 the SA model for the estimation of spatially distributed SWC. Because the TA model
597 was not worse than the SA model for the whole range of SWC, the TA model is
598 suggested for the estimation of spatially distributed SWC at different soil water
599 conditions.

600 Previous studies on SWC decomposition mainly focus on near surface layers
601 (Jawson and Niemann, 2007; Perry and Niemann, 2007, 2008; Joshi and Mohanty,
602 2010; Korres et al., 2010; Busch et al., 2012). This study decomposed spatiotemporal
603 SWC using the TA model for both the near surface and the root zone. The results
604 showed that the estimation of spatially distributed SWC at small watershed scales was
605 improved by the TA method that considers the $R_{tn}$. Because of the stronger time
606 stability of SWC in deeper soil layers (Biswas and Si, 2011), SWC evaluation in
607 thicker soil layers was more accurate than in shallow soil layers. This is particularly
608 important because SWC data for deeper soil layers in a watershed is more difficult to
609 collect than that of surface soil.

# 5 Conclusions

The TA model was used to decompose spatiotemporal SWC into time-stable patterns $M_{\hat{t}n}$, space-invariant temporal anomaly $A_{t\hat{n}}$, and space-variant temporal anomaly $R_{tn}$. This study indicated that underlying spatial patterns may exist in the $R_{tn}$ at small scales (e.g., small watersheds and hillslope) but may not at large scales such as the GENCAI network (~250 km²) in Italy. This was because the $R_{tn}$ at small scales was driven by "static" factors such as depth to the $CaCO_3$ layer and SOC at the Canadian site, while the $R_{tn}$ at large scales may be dominated by "dynamic" factors such as meteorological anomaly. Compared to the SA model, estimation of spatially distributed SWC was improved with the TA model at small watershed scales. This was because the TA model considered a fair amount of spatial variance in the $R_{tn}$, which was ignored in the SA model. Furthermore, the improved performance was observed mainly when soil water was drier or wetter than the average level, especially in drier conditions due to the high $\sigma_{\hat{n}}^2(R_{tn})$ value.

This study showed that outperformance of TA model over SA model is possible when $\sigma_{\hat{n}}^2(R_{tn})$ contributes substantial variance to the total variances of SWC, and significant spatial patterns (or EOFs) exist in the $R_{tn}$. Further application of the TA model for estimation of spatially distributed SWC at different scales and hydrological backgrounds is recommended. If the TA model parameters (i.e., $M_{\hat{t}n}$, EOF1 of the $R_{tn}$, and relationship between EC and $S_{t\hat{n}}$) are obtained from historical SWC dataset, a detailed spatially distributed SWC of near surface at watershed scales can be constructed from remote sensed SWC. Note that both models rely on previous SWC

632 measurements for model parameters. Therefore, the future study should be directed to
633 estimate spatially distributed SWC in un-gauged watersheds based on estimation of
634 model parameters using pedotransfer functions. Since the TA model needs one more
635 spatial parameter (i.e., $M_{\hat{t}n}$) than the SA model, advantage of the TA model may be
636 weakened. Nevertheless, the TA model may be preferred if it estimates spatial SWC
637 much better than the SA model such as at the dry conditions. The codes for
638 decomposing SWC with the SA and TA models and related EOF analysis were written
639 in Matlab and are freely available from the authors upon request.

640 ## Acknowledgements

641 The project was funded by the Natural Sciences and Engineering Research Council
642 (NSERC) of Canada. We thank Dr Asim Biswas, Dr Henry Wai Chau, Mr Trent
643 Pernitsky, and Mr Eric Neil for their help in data collection.

644 ## References

645 Biswas, A., Chau, H. W., Bedard-Haughn, A., and Si, B. C.: Factors controlling soil
646 water storage in the Hummocky landscape of the Prairie Pothole region of North
647 America, Can. J. Soil Sci., 92, 649–663, doi: 10.4141/CJSS2011-045, 2012.
648 Biswas, A. and Si, B. C.: Scales and locations of time stability of soil water storage in
649 a hummocky landscape, J. Hydrol., 408, 100–112, doi: 10.1016/j.jhydrol.2011.07.027,
650 2011.
651 Blöschl, G., Komma, J., and Hasenauer, S.: Hydrological downscaling of soil

652 moisture, Final report to the H-SAF (Hydrology Satellite Application Facility) via the
653 Austrian Central Institute for Meteorology and Geodynamics (ZAMG), Vienna
654 University of Technology, A-1040 Vienna, Austria, 2009.
655 Brocca, L., Melone, F., Moramarco, T., and Morbidelli, R.: Soil moisture temporal
656 stability over experimental areas in Central Italy, Geoderma, 148, 364–374, doi:
657 10.1016/j.geoderma.2008.11.004, 2009.
658 Brocca, L., Tullo, T., Melone, F., Moramarco, T., and Morbidelli, R.: Catchment scale
659 soil moisture spatial-temporal variability, J. Hydrol., 422-423, 63–75,
660 doi:10.1016/j.jhydrol.2011.12.039, 2012.
661 Brocca, L., Zucco, G., Mittelbach, H., Moramarco, T., and Seneviratne, S. I.: Absolute
662 versus temporal anomaly and percent of saturation soil moisture spatial variability for
663 six networks worldwide, Water Resour. Res., 50, 5560–5576, doi:
664 10.1002/2014WR015684, 2014.
665 Brocca, L., Zucco, G., Moramarco, T., and Morbidelli, R.: Developing and testing a
666 long-term soil moisture dataset at the catchment scale, J. Hydrol., 490, 144–151, doi:
667 10.1016/j.jhydrol.2013.03.029, 2013.
668 Burnham, K. P. and Anderson, D. R.: Model selection and multimodel inference: A
669 practical information-theoretic approach (2nd ed.), Springer-Verlag, New York, 2002.
670 Busch, F. A., Niemann, J. D., and Coleman, M.: Evaluation of an empirical
671 orthogonal function-based method to downscale soil moisture patterns based on
672 topographical attributes, Hydrol. Process., 26, 2696–2709, doi: 10.1002/hyp.8363,
673 2012.

674 Champagne, C., Berg, A. A., McNairn, H., Drewitt, G., and Huffman, T.: Evaluation
675 of soil moisture extremes for agricultural productivity in the Canadian prairies, Agric.
676 For. Meteorol., 165, 1–11, doi: 10.1016/j.agrformet.2012.06.003, 2012.
677 Famiglietti, J. S., Rudnicki, J. W., and Rodell, M.: Variability in surface moisture
678 content along a hillslope transect: Rattlesnake Hill, Texas, J. Hydrol., 210, 259–281,
679 doi: 10.1016/S0022-1694(98)00187-5, 1998.
680 Gómez-Plaza, A., Alvarez-Rogel, J., Albaladejo, J., and Castillo, V. M.: Spatial
681 patterns and temporal stability of soil moisture across a range of scales in a semi-arid
682 environment, Hydrol. Process., 14, 1261–1277, doi:
683 10.1002/(SICI)1099-1085(200005)14:7<1261::AID-HYP40>3.0.CO;2-D, 2000.
684 Gómez-Plaza, A., Martínez-Mena, M., Albaladejo, J., and Castillo, V. M.: Factors
685 regulating spatial distribution of soil water content in small semiarid catchments, J.
686 Hydrol., 253, 211–226, doi: 10.1016/S0022-1694(01)00483-8, 2001.
687 Grant, L., Seyfried, M., and McNamara, J.: Spatial variation and temporal stability of
688 soil water in a snow-dominated, mountain catchment, Hydrol. Process., 18,
689 3493–3511, doi: 10.1002/hyp.5789, 2004.
690 Grayson, R. B. and Western, A. W.: Towards areal estimation of soil water content
691 from point measurements: Time and space stability of mean response, J. Hydrol., 207,
692 68–82, doi: 10.1016/S0022-1694(98)00096-1, 1998.
693 Hu, W., Shao, M. A., Han, F. P., and Reichardt, K.: Spatio-temporal variability
694 behavior of land surface soil water content in shrub- and grass-land, Geoderma, 162,
695 260–272, doi: 10.1016/j.geoderma.2011.02.008, 2011.

696 Hu, W., Shao, M. A., and Reichardt, K.: Using a new criterion to identify sites for
697 mean soil water storage evaluation, Soil Sci. Soc. Am. J., 74, 762–773, doi:
698 10.2136/sssaj2009.0235, 2010.
699 Hu, W., Tallon, L. K., and Si, B. C.: Evaluation of time stability indices for soil water
700 storage upscaling, J. Hydrol., 475, 229–241, doi: 10.1016/j.jhydrol.2012.09.050,
701 2012.
702 Jawson, S. D. and Niemann, J. D.: Spatial patterns from EOF analysis of soil moisture
703 at a large scale and their dependence on soil, land-use, and topographic properties,
704 Adv. Water Resour., 30, 366–381, doi:10.1016/j.advwatres.2006.05.006, 2007.
705 Jia, Y. H. and Shao, M. A.: Temporal stability of soil water storage under four types of
706 revegetation on the northern Loess Plateau of China, Agric. Water Manage., 117,
707 33–42, doi: 10.1016/j.agwat.2012.10.013, 2013.
708 Johnson, R. A. and Wichern, D. W.: Applied multivariate statistical analysis, Prentice
709 Hall, Upper Saddle River, New Jersey, 2002.
710 Joshi, C. and Mohanty, B. P.: Physical controls of near-surface soil moisture across
711 varying spatial scales in an agricultural landscape during SMEX02, Water Resour.
712 Res., 46, doi: 10.1029/2010WR009152, 2010.
713 Korres, W., Koyama, C. N., Fiener, P., and Schneider, K.: Analysis of surface soil
714 moisture patterns in agricultural landscapes using Empirical Orthogonal Functions,
715 Hydrol. Earth Syst. Sci., 14, 751–764, doi: 10.5194/hess-14-751-2010, 2010.
716 Martínez-Fernández, J. and Ceballos, A.: Temporal stability of soil moisture in a
717 large-field experiment in Spain, Soil Sci. Soc. Am. J., 67, 1647–1656, 2003.

718 Millar, J. B.: Shoreline-area ratios as a factor in rate of water loss from small sloughs,
719 J. Hydrol., 14, 259–284, doi: 10.1016/0022-1694(71)90038-2, 1971.
720 Mittelbach, H. and Seneviratne, I.: A new perspective on the spatio-temporal
721 variability of soil moisture: Temporal dynamics versus time-invariant contributions,
722 Hydrol. Earth Syst. Sci., 16, 2169–2179, doi: 10.5194/hess-16-2169-2012, 2012.
723 Mohanty, B. P. and Skaggs, T. H.: Spatio-temporal evolution and time–stable
724 characteristics of soil moisture within remote sensing footprints with varying soil
725 slope and vegetation, Adv. Water Resour., 24, 1051–1067, doi:
726 10.1016/S0309-1708(01)00034-3, 2001.
727 Peel, M. C., Finlayson, B. L., and McMahon, T. A.: Updated world map of the
728 Köppen-Geiger climate classification, Hydrol. Earth Syst. Sci., 11, 1633–1644,
729 doi:10.5194/hess-11-1633-2007, 2007.
730 Perry, M. A. and Niemann J. D.: Analysis and estimation of soil moisture at the
731 catchment scale using EOFs, J. Hydrol., 334, 388–404, doi:
732 10.1016/j.jhydrol.2006.10.014, 2007.
733 Perry, M. A. and Niemann J. D.: Generation of soil moisture patterns at the catchment
734 scale by EOF interpolation, Hydrol. Earth Syst. Sci., 12, 39–53,
735 doi:10.5194/hess-12-39-2008, 2008.
736 Robinson, D. A., Campbell, C. S., Hopmans, J. W., Hornbuckle, B. K., Jones, S. B.,
737 Knight, R., Ogden, F., Selker, J., and Wendroth, O.: Soil moisture measurement for
738 ecological and hydrological watershed-scale observatories: A review, Vadose Zone J.,
739 7, 358–389, doi: 10.2136/vzj2007.0143, 2008.

740 Rötzer, K., Montzka, C., and Vereecken, H.: Spatio-temporal variability of global soil
741 moisture products, J. Hydrol., 522, 187–202, doi: 10.1016/j.jhydrol.2014.12.038,
742 2015.
743 She, D. L., Liu, D. D., Peng, S. Z., and Shao, M. A.: Multiscale influences of soil
744 properties on soil water content distribution in a watershed on the Chinese Loess
745 Plateau, Soil Sci., 178, 530–539, doi: 10.1016/j.jhydrol.2014.08.034, 2013a.
746 She, D. L., Xia, Y. Q., Shao, M. A., Peng, S. Z., and Yu, S. E.: Transpiration and
747 canopy conductance of Caragana Korshinskii trees in response to soil moisture in
748 sand land of China, Agrofor. Syst., 87, 667–678, doi: 10.1007/s10457-012-9587-4,
749 2013b.
750 Sherratt, D. J. and Wheater, H. S.: The use of surface-resistance soil-moisture
751 relationships in soil-water budget models, Agric. For. Meteorol., 31, 143–157, doi:
752 10.1016/0168-1923(84)90016-9, 1984.
753 Soil Survey Staff: Soil Taxonomy, 11th edition, USDA National Resources
754 Conservation Services, Washington DC, 2010.
755 Starr, G. C.: Assessing temporal stability and spatial variability of soil water patterns
756 with implications for precision water management, Agric. Water Manage., 72,
757 223–243, doi: 10.1016/j.agwat.2004.09.020, 2005.
758 Vachaud, G., De Silans, A. P., Balabanis, P., and Vauclin, M.: Temporal stability of
759 spatially measured soil water probability density function, Soil Sci. Soc. Am. J., 49,
760 822–828, 1985.
761 van der Kamp, G., Hayashi, M., and Gallen, D.: Comparing the hydrology of grassed

762 and cultivated catchments in the semi-arid Canadian prairies, Hydrol. Process., 17,
763 559–575, doi: 10.1002/hyp.1157, 2003.
764 Vanderlinden, K., Vereecken, H., Hardelauf, H., Herbst, M., Martinez, G., Cosh, M.
765 H., and Pachepsky, Y. A.: Temporal stability of soil water contents: A review of data
766 and analyses, Vadose Zone J., 11, 4, doi: 10.2136/vzj2011.0178, 2012.
767 Vereecken, H., Kamai, T., Harter, T., Kasteel, R., Hopmans, J., and Vanderborght, J.:
768 Explaining soil moisture variability as a function of mean soil moisture: A stochastic
769 unsaturated flow perspective, Geophys. Res. Lett., 34, L22402, doi:
770 10.1029/2007GL031813, 2007.
771 Venkatesh, B., Nandagiri, L., Purandara, B. K., and Reddy, V. B.: Modelling soil
772 moisture under different land covers in a sub-humid environment of Western Ghats,
773 India, J. Earth Syst. Sci., 120, 387–398, 2011.
774 Walsh, J. E. and Mostek, A.: A quantitative-analysis of meteorological anomaly
775 patterns over the United-States, 1900–1977, Mon. Weather Rev., 108, 615–630, doi:
776 10.1175/1520-0493(1980)108<0615:AQAOMA>2.0.CO;2, 1980.
777 Wang, Y. Q., Shao, M. A., Liu. Z. P., and Warrington, D. N.: Regional spatial pattern
778 of deep soil water content and its influencing factors, Hydrolog. Sci. J., 57, 265–281,
779 doi: 10.1080/02626667.2011.644243, 2012.
780 Ward, P. R., Flower, K. C., Cordingley, N., Weeks, C., and Micin, S. F.: Soil water
781 balance with cover crops and conservation agriculture in a Mediterranean climate,
782 Field Crop. Res., 132, 33–39, doi: 10.1016/j.fcr.2011.10.017, 2012.
783 Zhao, Y., Peth, S., Wang, X. Y., Lin, H., and Horn, R.: Controls of surface soil

784 moisture spatial patterns and their temporal stability in a semi-arid steppe, Hydrol.
785 Process., 24, 2507–2519, doi: 10.1002/hyp.7665, 2010.

## Figure captions

**Figure 1.** Decomposition of spatiotemporal soil water content (SWC) in different models.

**Figure 2.** Daily mean air temperature and precipitation during the study period.

**Figure 3.** Components of soil water content in (a) the SA model (spatial mean soil water content $S_{t\hat{n}}$ and spatial anomaly $Z_{tn}$) and in (b) the TA model (time-stable pattern $M_{\hat{t}n}$, space-invariant temporal anomaly $A_{t\hat{n}}$, and space-variant temporal anomaly $R_{tn}$) for 0–0.2 and 0–1.0 m. Also shown is the elevation.

**Figure 4.** (a) The EOF1 of the spatial anomaly $Z_{tn}$ and (b) relationships of associated EC1 versus spatial mean soil water content $Z_{tn}$ fitted by the cosine function (Eq. 4).

**Figure 5.** Spatial variances of different components in Eq. (8) expressed in $\%^2$ (upper panel) and as percentage (lower panel) for (a) 0–0.2 and (b) 0–1.0 m. Spatial mean soil water content $S_{t\hat{n}}$ on each measurement day is also shown.

**Figure 6.** (a) The EOF1 of the space-variant temporal anomaly $R_{tn}$ and (b) relationships of associated EC1 versus spatial mean soil water content $S_{t\hat{n}}$ fitted by the cosine function (Eq. 4).

**Figure 7.** Estimated soil water content (SWC) versus measured SWC for three dates at different soil water conditions (23 August 2008, 27 October 2009, and 13 May 2011 are associated with relatively dry, medium, and wet days, respectively) using the TA model for (a) 0–0.2 and (b) 0–1.0 m.

**Figure 8.** The Nash-Sutcliffe coefficient of efficiency (NSCE) of soil water content

estimation using the TA and SA models for (a) 0–0.2 and (b) 0–1.0 m for both cross validation (CV) and external validation (EV). At 0–0.2 m, negative Nash-Sutcliffe coefficient of efficiency values for three dates (22 October 2008, 27 August 2009, and 27 October 2009) are not shown. Spatial mean soil water content $S_{t\hat{n}}$ on each measurement day is also shown.

**Figure 9.** Difference between the Nash-Sutcliffe coefficient of efficiency (NSCE) of soil water content estimation by both cross validation (CV) and external validation (EV) using the TA and SA models as a function of space-invariant temporal anomaly $A_{t\hat{n}}$ for (a) 0–0.2 and (b) 0–1.0 m.

**Figure 10.** Difference between the Nash-Sutcliffe coefficient of efficiency (NSCE) of soil water content evaluation by the cross validation using the TA and SA models as a function of space-invariant temporal anomaly $A_{t\hat{n}}$ for (a) 0–0.06 m of the Chinese Loess Plateau hillslope and (b) 0–0.15 m of the GENCAI network in Italy.

**Table 1.** Pearson correlation coefficients between time-stable pattern $M_{\hat{t}n}$, EOF1 of space-variant temporal anomaly $R_{tn}$ and various properties.

| | 0–0.2 m | | 0–1.0 m | |
|---|---|---|---|---|
| | $M_{\hat{t}n}$ | EOF1 | $M_{\hat{t}n}$ | EOF1 |
| Sand content | -0.52** | -0.36** | -0.66** | -0.26** |
| Silt content | 0.29** | 0.14 | 0.40** | 0.06 |
| Clay content | 0.43** | 0.38** | 0.51** | 0.33** |
| Organic carbon | 0.78** | 0.83** | 0.73** | 0.76** |
| Wetness index | 0.64** | 0.59** | 0.68** | 0.56** |
| Depth to $CaCO_3$ layer | 0.77** | 0.84** | 0.65** | 0.88** |
| A horizon depth | 0.51** | 0.62** | 0.44** | 0.65** |
| C horizon depth | 0.66** | 0.69** | 0.58** | 0.76** |
| Bulk density | -0.58** | -0.67** | -0.46** | -0.62** |
| Elevation | -0.24** | -0.28** | -0.24** | -0.32** |
| Specific contributing area | 0.20* | 0.24** | 0.24** | 0.23** |
| Convergence index | -0.58** | -0.56** | -0.55** | -0.58** |
| Curvature | -0.10 | -0.08 | -0.19* | -0.16 |
| Cos(aspect) | 0.05 | 0.04 | 0.08 | 0.05 |
| Gradient | -0.12 | -0.09 | -0.21* | -0.02 |
| Slope | -0.51** | -0.48** | -0.56** | -0.44** |
| Upslope length | 0.19* | 0.21* | 0.21* | 0.25** |
| Solar radiation | -0.07 | 0.03 | -0.11 | 0.08 |
| Flow connectivity | 0.45** | 0.43** | 0.49** | 0.49** |
| Leaf area index | -0.07 | 0.06 | -0.10 | -0.14 |
| Variance explained[1] | 74.5% | 81.6% | 75.6% | 81.0% |

[1]percent of variance explained by the controlling factors obtained by the multiple stepwise regressions.
*Significant at $P<0.05$; ** Significant at $P<0.01$.

**Table A1.** Notations.

| | |
|---|---|
| $M_{\hat{t}\hat{n}}$ | spatial mean of $M_{\hat{t}n}$ |
| $R_{tn}$ | space-variant temporal anomaly of SWC at location *n* and time *t* |
| $A_{t\hat{n}}$ | space-invariant temporal anomaly of SWC at time *t* |
| $Z_{tn}$ | spatial anomaly of SWC at location *n* and time *t* |
| $S_{t\hat{n}}$ | spatial mean SWC at time *t* |
| $\sigma^2_{\hat{n}}$ | spatial variance |
| $A_{tn}$ | temporal anomaly of SWC at location *n* and time *t* |
| $\delta_{\hat{t}n}$ | temporal mean relative difference of SWC at location *n* |
| cov | spatial covariance |
| $S_{tn}$ | SWC at location *n* and time *t* |
| $M_{\hat{t}n}$ | time-stable pattern of SWC |
| ECs | temporally-varying coefficients of $R_{tn}$ (or $Z_{tn}$) |
| EOFs | time-invariant spatial structures of $R_{tn}$ (or $Z_{tn}$) |
| NSCE | Nash-Sutcliffe coefficient of efficiency |
| *R* | Pearson correlation coefficient |
| SWC | soil water content |

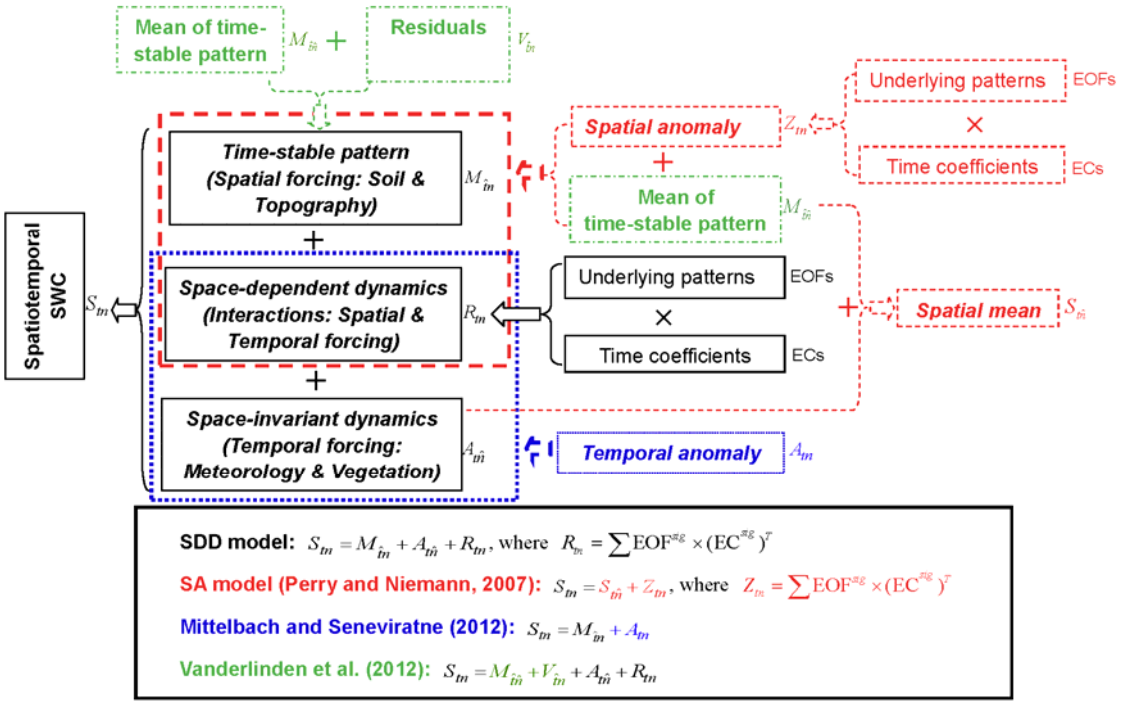
Mean of time-stable pattern
Residuals
Time-stable pattern (Spatial forcing: Soil & Topography)
Space-dependent dynamics (Interactions: Spatial & Temporal forcing)
Space-invariant dynamics (Temporal forcing: Meteorology & Vegetation)
Spatiotemporal SWC
Spatial anomaly
Mean of time-stable pattern
Underlying patterns
EOFs
Time coefficients
ECs
Spatial mean
Temporal anomaly
SDD model: $S_{tn} = M_{\hat{t}n} + A_{t\hat{n}} + R_{tn}$, where $R_{tn} = \sum \mathrm{EOF}^{reg} \times (\mathrm{EC}^{reg})^T$
SA model (Perry and Niemann, 2007): $S_{tn} = S_{t\hat{n}} + Z_{tn}$, where $Z_{tn} = \sum \mathrm{EOF}^{reg} \times (\mathrm{EC}^{reg})^T$
Mittelbach and Seneviratne (2012): $S_{tn} = M_{\hat{t}n} + A_{tn}$
Vanderlinden et al. (2012): $S_{tn} = M_{\hat{t}n} + V_{\hat{t}n} + A_{t\hat{n}} + R_{tn}$

Fig. 1

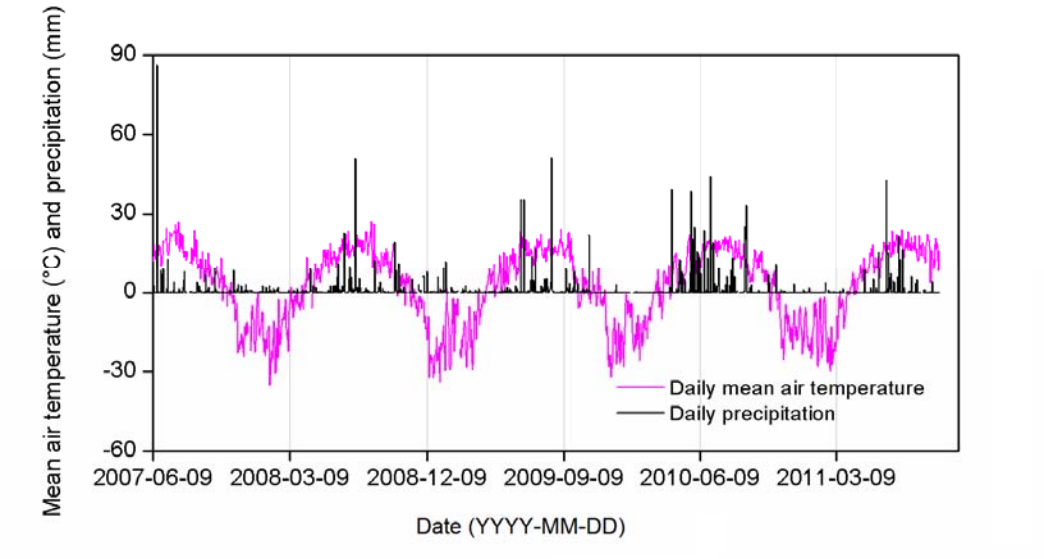
Mean air temperature (°C) and precipitation (mm)
90
60
30
0
-30
-60
2007-06-09
2008-03-09
2008-12-09
2009-09-09
2010-06-09
2011-03-09
Date (YYYY-MM-DD)
Daily mean air temperature
Daily precipitation

Fig. 2

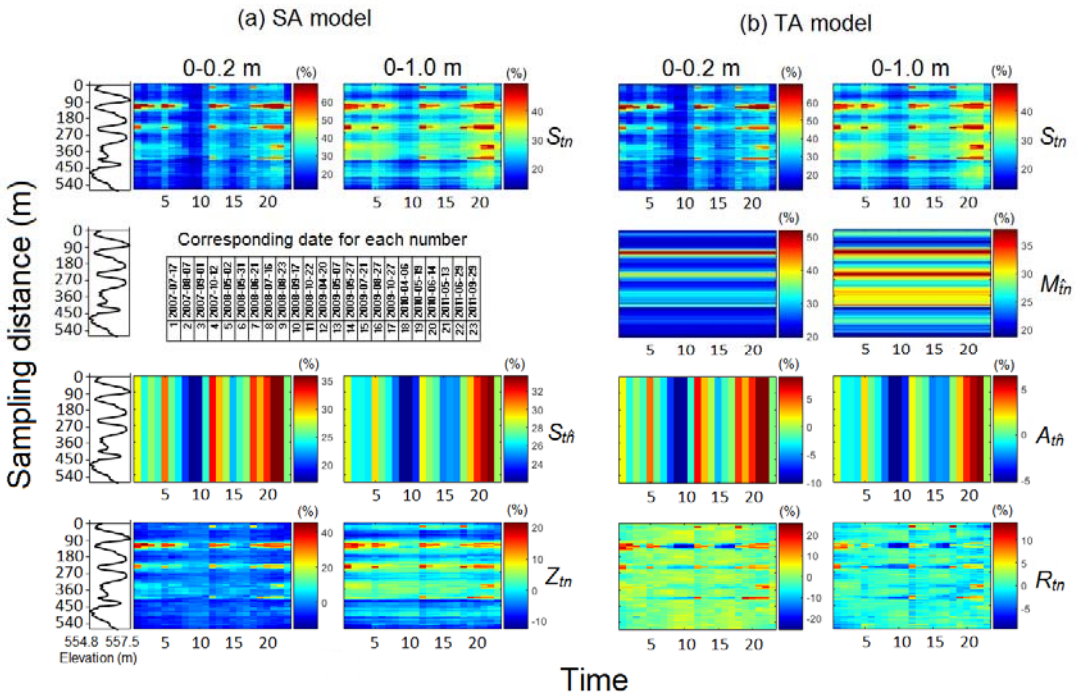
(a) SA model
(b) TA model
0-0.2 m
0-1.0 m
Sampling distance (m)
Corresponding date for each number
Time
Elevation (m)

Fig. 3

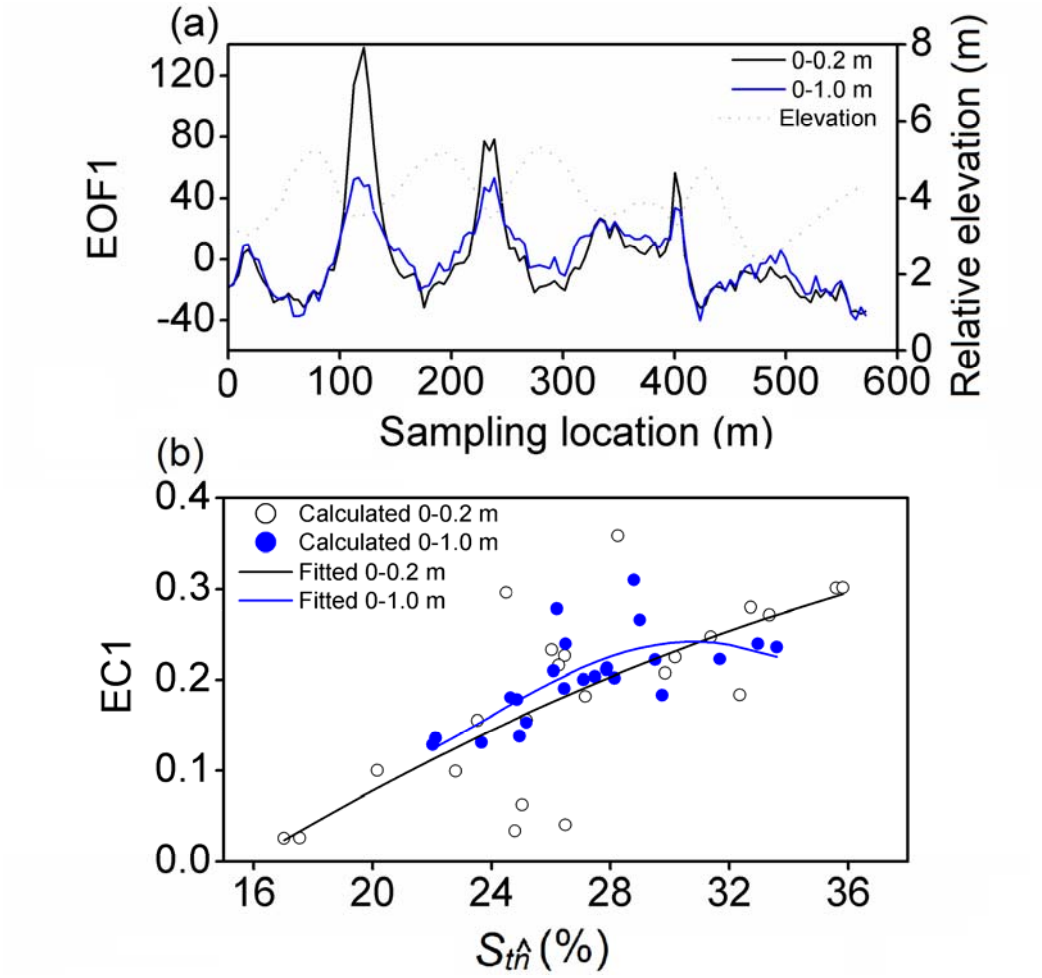
(a)
EOF1
Relative elevation (m)
0-0.2 m
0-1.0 m
Elevation
Sampling location (m)
(b)
EC1
Calculated 0-0.2 m
Calculated 0-1.0 m
Fitted 0-0.2 m
Fitted 0-1.0 m
$S_{th}$ (%)

Fig. 4

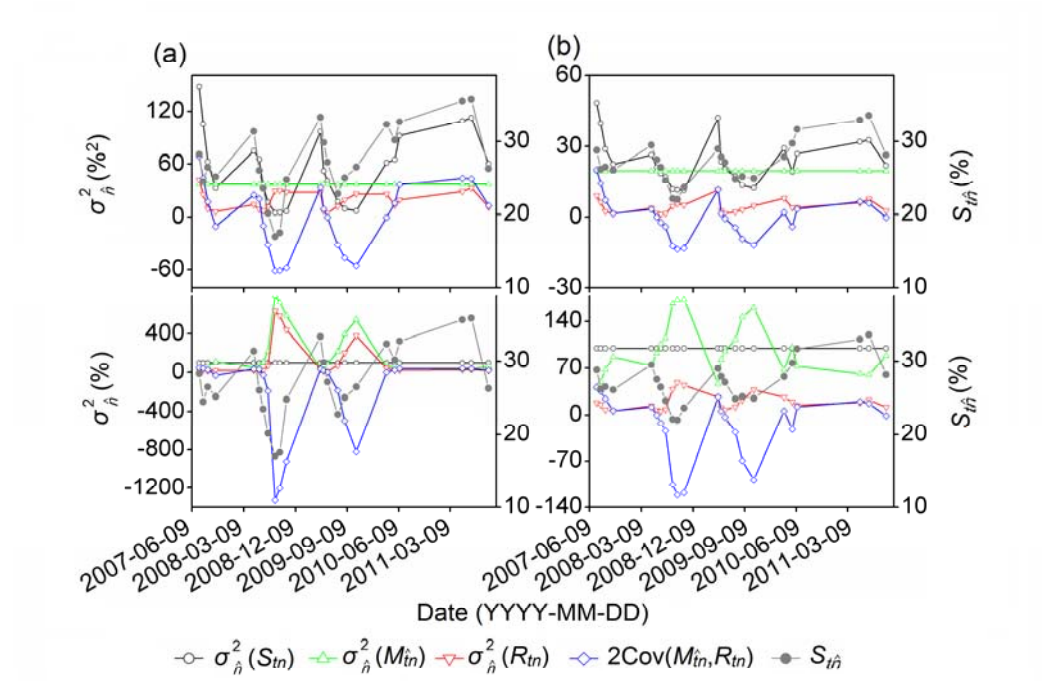
(a)
(b)
Date (YYYY-MM-DD)
2007-06-09
2008-03-09
2008-12-09
2009-09-09
2010-06-09
2011-03-09
2Cov(M_tn,R_tn)

Fig. 5

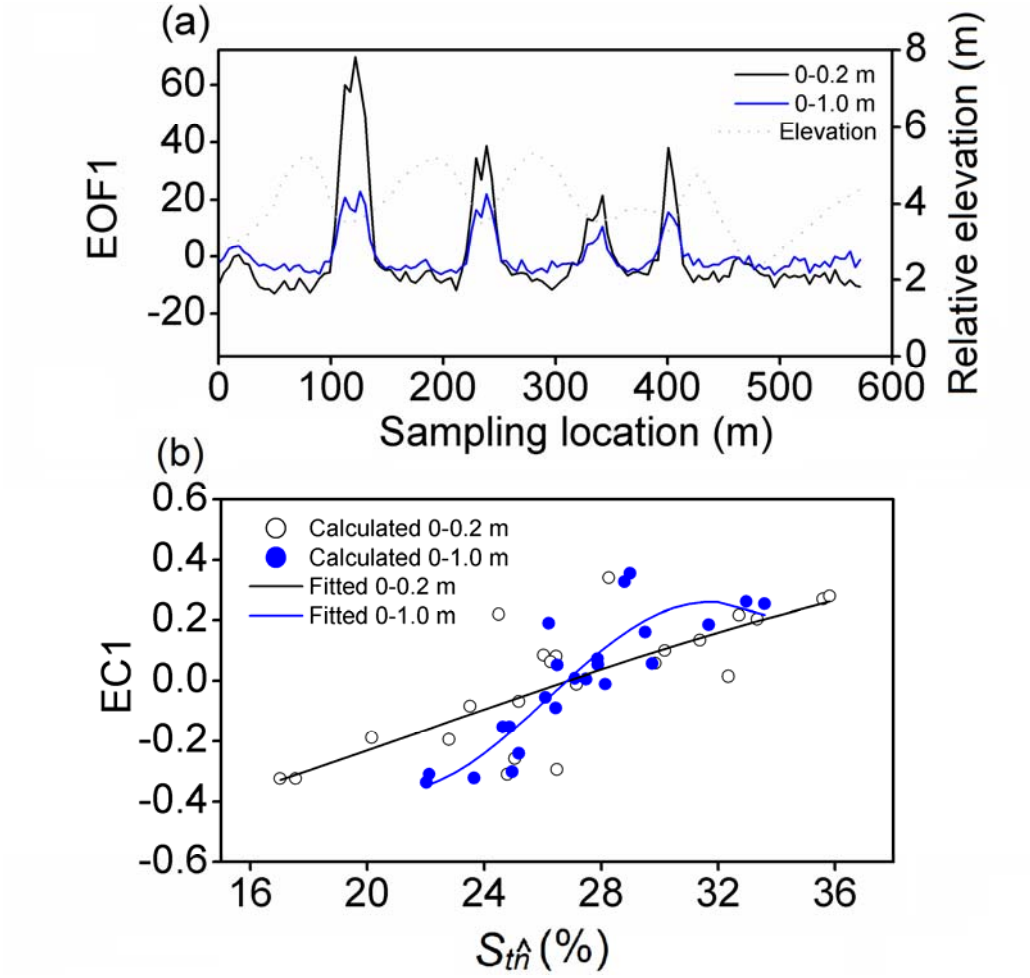
(a)
EOF1
Relative elevation (m)
0-0.2 m
0-1.0 m
Elevation
Sampling location (m)
(b)
EC1
Calculated 0-0.2 m
Calculated 0-1.0 m
Fitted 0-0.2 m
Fitted 0-1.0 m
$S_{th}$ (%)

Fig. 6

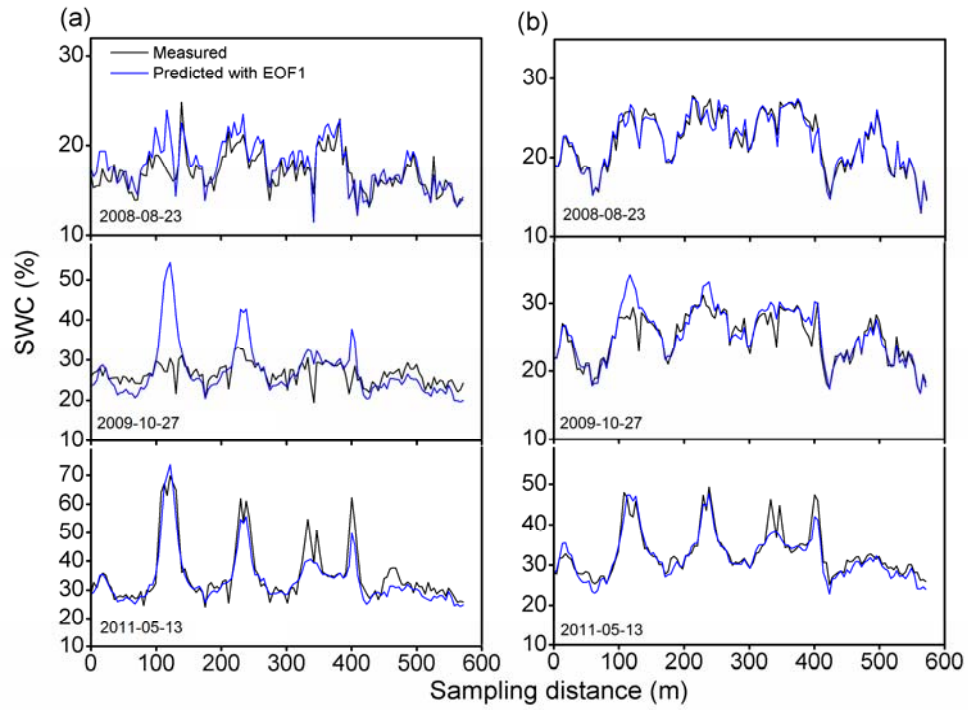
(a)
(b)
Measured
Predicted with EOF1
2008-08-23
2009-10-27
2011-05-13
SWC (%)
Sampling distance (m)

Fig. 7

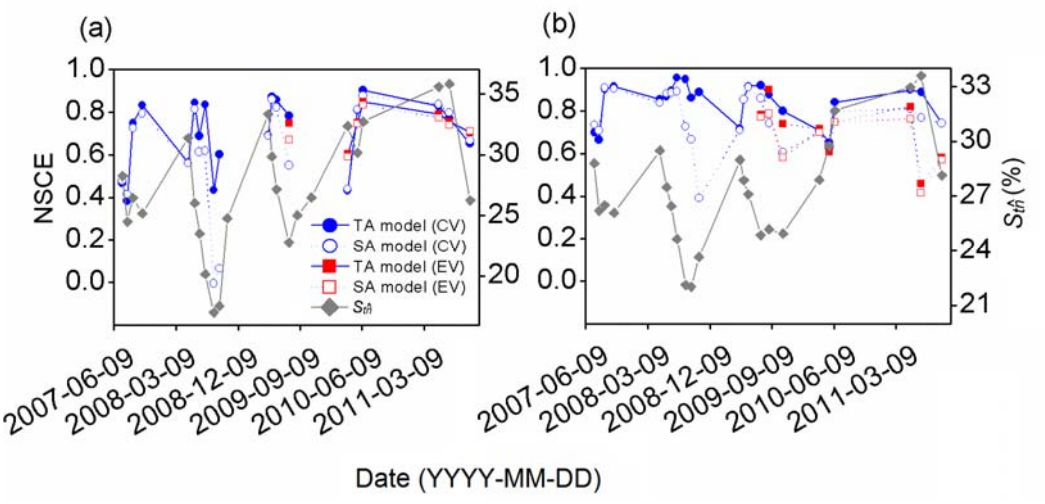
(a)
(b)
NSCE
$S_{th}$ (%)
TA model (CV)
SA model (CV)
TA model (EV)
SA model (EV)
$S_{th}$
2007-06-09
2008-03-09
2008-12-09
2009-09-09
2010-06-09
2011-03-09
Date (YYYY-MM-DD)

Fig. 8

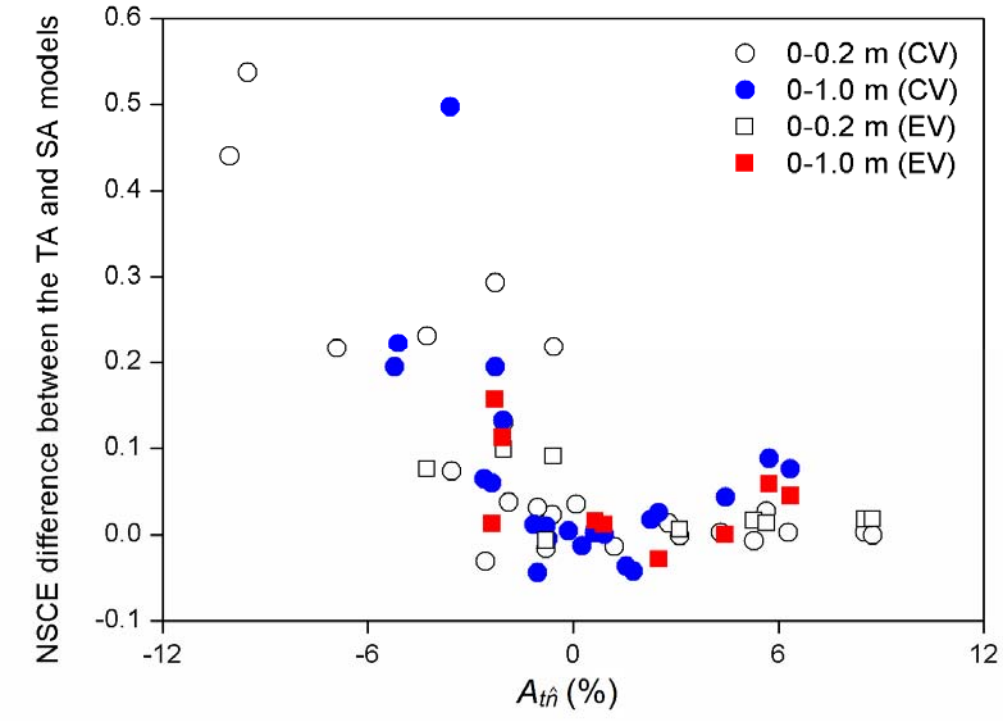
NSCE difference between the TA and SA models
0.6
0.5
0.4
0.3
0.2
0.1
0.0
-0.1
-12
-6
0
6
12
$A_{t\hat{n}}$ (%)
0-0.2 m (CV)
0-1.0 m (CV)
0-0.2 m (EV)
0-1.0 m (EV)

Fig. 9

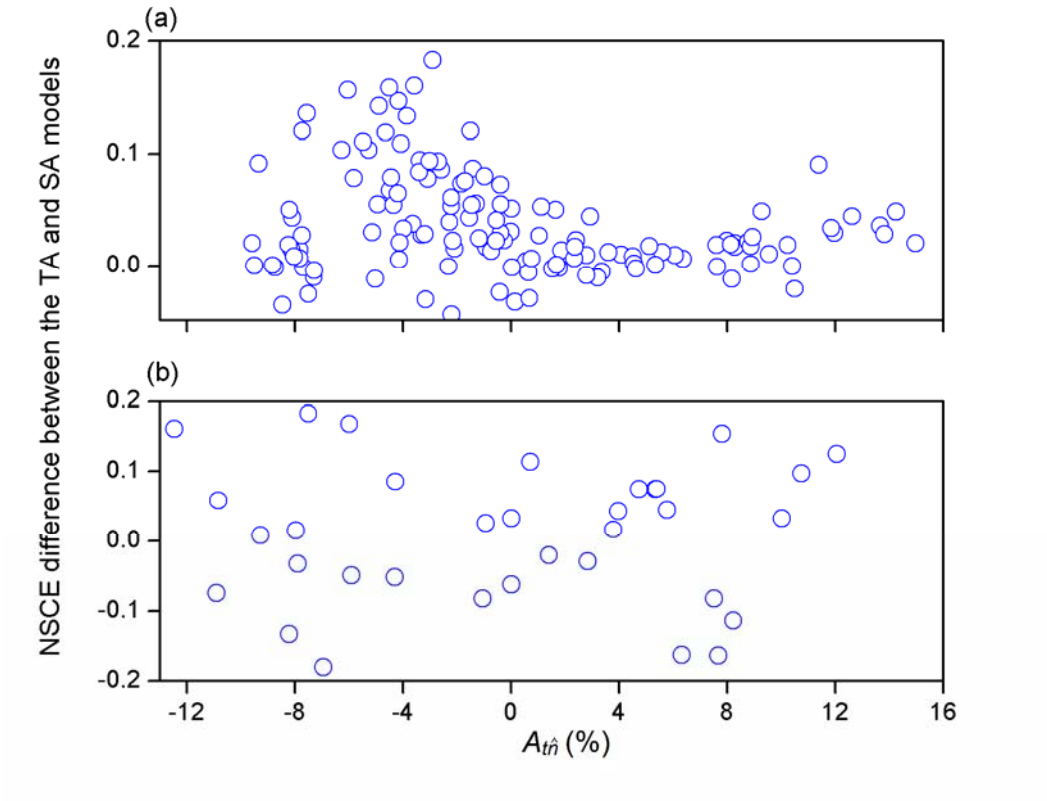
(a)
(b)
0.2
0.1
0.0
-0.1
-0.2
-12
-8
-4
0
4
8
12
16
NSCE difference between the TA and SA models
$A_{t\hat{n}}$ (%)

Fig. 10